

# Conformal and $k$ NN Predictive Uncertainty Quantification Algorithms in Metric Spaces

Gábor Lugosi<sup>1,2,3</sup> and Marcos Matabuena<sup>\*4,5</sup>

<sup>1</sup>Department of Economics and Business, Pompeu Fabra University, Barcelona, Spain

<sup>2</sup>ICREA, Pg. Lluís Companys 23, 08010 Barcelona, Spain

<sup>3</sup>Barcelona Graduate School of Economics

<sup>4</sup>Department of Biostatistics, Harvard University, Boston, MA 02115, USA

<sup>5</sup>Universidad de Santiago de Compostela

## Abstract

This paper introduces a framework for uncertainty quantification in regression models defined in metric spaces. Leveraging a newly defined notion of homoscedasticity, we develop a conformal prediction algorithm that offers finite-sample coverage guarantees and fast convergence rates of the oracle estimator. In heteroscedastic settings, we forgo these non-asymptotic guarantees to gain statistical efficiency, proposing a local  $k$ -nearest-neighbor method without conformal calibration that is adaptive to the geometry of each particular nonlinear space. Both procedures work with any regression algorithm and are scalable to large data sets, allowing practitioners to plug in their preferred models and incorporate domain expertise. We prove consistency for the proposed estimators under minimal conditions. Finally, we demonstrate the practical utility of our approach in personalized-medicine applications involving random response objects such as probability distributions and graph Laplacians.

**Keywords:** Digital Health; Uncertainty Quantification; Metric Spaces; Conformal Prediction; Fréchet Mean; Personalized medicine applications.

## 1 Introduction

### 1.1 Motivation and goal

The increasing use of statistical and machine-learning algorithms is transforming healthcare, finance, and digital markets [Banerji et al., 2023, Hammouri et al., 2023, Matabuena, 2022]. It has become more critical than ever to conduct uncertainty analysis to create trustworthy predictive models and validate their usefulness [Romano et al., 2019]. Data analysts tend to

---

\*matabuena@hsph.harvard.edu

\* Corresponding author. Email: matabuena@hsph.harvard.edu

focus on pointwise estimation through the conditional mean between a response and a set of predictors, neglecting other crucial aspects of the conditional distribution between the involved random variables [Kneib et al., 2021]. In order to quantify the uncertainty of the point estimates, we need to estimate other characteristics of the conditional distribution beyond the conditional mean.

An innovative approach to tackle uncertainty quantification problems involves employing the conformal inference framework, first introduced by Gammerman, Vovk, and Vapnik (see [Gammerman et al., 1998]). Building upon this foundation, Vovk, Gammerman, and Shafer have made significant contributions to the field [Vovk et al., 2005]. Conformal inference allows one to construct prediction sets with non-asymptotic guarantees, setting it apart from other methods that only offer asymptotic guarantees.

However, despite its attractive properties and advantages, conformal inference does have some limitations that include:

1. **Computational Complexity:** The implementation of conformal inference methods can be computationally expensive, especially if data-splitting strategies to estimate the underlying regression model and prediction region (referred to as *conformal-split* in the literature) are not considered [Vovk et al., 2018, Solari and Djordjilović, 2022].
2. **Conservative Intervals:** The method tends to produce conservative intervals if the regression function used is not well-calibrated with respect to the underlying model, or if the conformal inference method is misspecified [Lu, 2023] (e.g., using a homoscedastic model when the underlying conditional distribution function between the random response variable  $Y$  and the random predictor  $X$  is governed by heteroscedastic random errors).
3. **Limited Applicability:** Conformal inference may have limited applicability, particularly in scenarios with multivariate responses or when the observed data is extracted from complex survey designs where the exchangeability hypothesis is violated (see Barber et al. [2023], who quantify the impact of this fact in terms of the total variation distance between distributions).
4. **Asymptotic Guarantees:** In some special cases, other methods may provide stronger asymptotic guarantees compared to the algorithms derived for the conformal inference framework (see Györfi and Walk [2019] for a discussion).

Related to this, a fascinating and still under-explored question in the predictive-inference literature is how conformalizing an algorithm impacts its statistical efficiency. Vovk dubbed this general mathematical challenge the Burnaev-Wasserman program (see Vovk et al. [2022]). Evidence from scalar-response settings and certain heteroscedastic scenarios suggests that conformal prediction can underperform in terms of conditional coverage calibration; for instance, this occurs when using bootstrap-predictive methods Zhang [2022]. This limitation becomes even more pronounced with high-dimensional responses or when the goal is to predict metric-space-valued responses. In such situations, the quality of the estimates tend to degrade more quickly. Consequently, the requirement of non-asymptotic coverage guarantees typically yields more conservative prediction regions. As a result, conformal prediction regions may substantially deviate from the population-prediction region, leading to a marked reduction in statistical efficiency for finite samples in terms of conditional coverage.

In the context of precision and digital medicine, clinical outcomes can take on complex statistical forms as random objects, such as probability distributions or graphs [Matabuena, 2022]. For instance, in the case of a glucose time series, a modern approach to summarizing the glucose

profiles involves using a distributional representation of the time series, such as their quantile functions. As prior research has shown, these new representations [Ghosal and Matabuena, 2023] can capture information about glucose homeostasis metabolism that traditional diabetes biomarkers cannot measure [Matabuena et al., 2021a, 2022a, Ghosal et al., 2021a].

For all these reasons, there is need for new predictive inference methods for regression models defined in metric spaces. To the best of our knowledge, the only approach that directly tackles predictive uncertainty quantification is the method of Zhou and Müller [2024], which appeared on arXiv at the same time as an earlier draft of the present work [Lugosi and Matabuena, 2024]. Zhou and Müller introduced a model-free conformal-inference procedure based on a conditional data depth-called the *distance profile*. Their paper is a generalization to metric spaces of a scalar distributional split-conformal method of Chernozhukov et al. [2021a]. However, the scalar procedure of Chernozhukov et al. [2021a] relies on estimating the conditional distribution of several quantities and achieves fast rates only when that distribution can be well approximated by parametric or semiparametric models-an assumption rarely tenable in high-dimensional or metric-response problems. To alleviate this difficulty, the method of Zhou and Müller [2024] imposes differentiability conditions that restrict applicability to discrete or otherwise non-smooth metric spaces. They also require multiple data splits to preserve finite-sample conformal guarantees, and their theory is limited to a single univariate Euclidean covariate, leading to slow convergence in some scenarios.

In multivariate settings, the method continues to depend on kernel-smoothing estimators. However, to mitigate the curse of dimensionality, it aggregates all predictors into a single-index model, which increases the rigidity of the final model. Moreover, its reliance on smoothness assumptions limits applicability to mixed continuous discrete covariates, as commonly encountered in physical-activity monitoring or survey-based medical data.

Motivated by these shortcomings and by the loss of efficiency observed in existing conformal algorithms in high-dimensional response spaces, we propose a general uncertainty-quantification framework for regression on separable metric spaces (see Fréchet [1948], Petersen and Müller [2019], Schötz [2021]). Noting that conformal prediction incurs a smaller efficiency loss under homoscedasticity, we introduce a new notion of homoscedasticity tailored to metric spaces and design conformal algorithms that estimate the regression function directly in that setting, attaining fast convergence rates. For heteroscedastic data, we propose a local  $k$ -nearest-neighbour conformal method that adapts naturally to non-linear geometric structure and scales to large data sets. Both procedures work with any regression algorithm, remain computationally efficient for large samples, and are shown to be consistent under some assumptions-often weaker than those required in the Euclidean literature, which is a special case of our framework. We demonstrate the practical value of the methodology in personalised medicine applications where the responses are probability distributions or Laplacian graphs.

Below, we introduce the notation and mathematical concepts to define the new uncertainty quantification framework.

## 1.2 Notation and problem definition

Let  $(X, Y) \in \mathcal{X} \times \mathcal{Y}$  be a pair of random variables that play the role of the predictor and response variable in a regression model. Our predictive uncertainty quantification algorithms handle both predictors and responses in general metric spaces. For simplicity, however, we assume that  $\mathcal{X} = \mathbb{R}^p$  and  $\mathcal{Y}$  is a separable metric space equipped with a distance  $d_1$ . We assume that there exists  $y \in \mathcal{Y}$  such that  $\mathbb{E}(d_1^2(Y, y)) < \infty$ . The regression function  $m$  is defined as

$$m(x) = \operatorname{argmin}_{y \in \mathcal{Y}} \mathbb{E}(d_1^2(Y, y) | X = x), \quad (1)$$

where  $x \in \mathbb{R}^p$ . In other words,  $m$  is the conditional Fréchet mean [Petersen and Müller, 2019]. For simplicity, we assume that the minimum in (1) is achieved for each  $x$  and moreover, the conditional Fréchet mean of  $Y$  given  $X = x$ , is unique. We note here that one may also consider the conditional Fréchet median obtained by  $\operatorname{argmin}_{y \in \mathcal{Y}} \mathbb{E}(d_1(Y, y) | X = x)$ . However, this is a special case of our setup obtained by replacing the metric  $d_1$ , by  $\sqrt{d_1}$  (which is also a metric). Suppose that  $\mathcal{Y}$  is also equipped with another distance  $d_2$ . We may have  $d_2 = d_1$ , but in some cases it is convenient to work with two distances.

For  $y \in \mathcal{Y}$  and  $r \geq 0$ , denote by  $\mathcal{B}(y, r) := \{z \in \mathcal{Y}; d_2(y, z) \leq r\}$ , the closed ball of center  $y \in \mathcal{Y}$ , and radius  $r$ .

**Remark 1.**  $d_1$  denote the metric used in the loss function used to obtain the regression function  $m$ , and  $d_2$ , possibly distinct from  $d_1$ , denotes the metric employed to derive the final prediction region. Allowing  $d_1 \neq d_2$  offers additional modelling flexibility:  $d_1$  can capture the application-specific geometry of the response space, whereas selecting a simpler metric for  $d_2$ —for example, the supremum norm—often simplifies both the computation and the visualisation of the resulting prediction sets, particularly in high- or infinite-dimensional settings.

We now introduce the notion of *homoscedasticity* for the random pair  $(X, Y)$ . The differentiation between homoscedasticity and heteroscedasticity is critical for our subsequent analysis. Based on the notion of *homoscedasticity*, we can obtain conformal prediction algorithms that are statistically efficient in general metric spaces.

**Definition 1.** We say that the distribution of  $(X, Y)$  is homoscedastic with respect to the regression function  $m$  if there exists a function  $\phi : [0, \infty) \rightarrow [0, 1]$  such that for all  $x \in \mathbb{R}^p$  and  $r \geq 0$ ,

$$\mathbb{P}(Y \in \mathcal{B}(m(x), r) | X = x) = \phi(r).$$

To motivate better our definition of homoscedasticity, let us consider the following examples. The first example is the most natural and commonly encountered in the statistical literature. In this case, the notion of homoscedasticity aligns with the traditional definition.

However, the second example is non-trivial and serves to illustrate that even in a spaces without a vector-space structure, it is still possible to have statistical models that fall under the homoscedastic regime according to our definition.

**Example 1.** Suppose that  $\mathcal{X} = \mathbb{R}^p$ ,  $\mathcal{Y} = \mathbb{R}^m$ ,  $d_1(\cdot, \cdot) = d_2(\cdot, \cdot) = \|\cdot - \cdot\|$  (arbitrary norm in  $\mathbb{R}^m$ ), and consider the regression model

$$Y = f(X) + \varepsilon, \quad (2)$$

where the random vector  $\varepsilon$ , taking values in  $\mathbb{R}^m$ , is independent of  $X$ , and satisfies  $\mathbb{E}(\varepsilon) = 0$ . It is easy to check that  $m = f$ .

Obviously,  $\mathbb{P}(d_2(Y, m(x)) \leq r | X = x) = \mathbb{P}(\|\varepsilon\| \leq r | X = x) = \phi(r)$ , due to the independence of  $\varepsilon$  and  $X$ .

**Example 2.** Consider  $\mathcal{X} = \mathbb{R}^p$  and  $\mathcal{Y} = \mathcal{W}_2(\mathbb{R})$ , where  $\mathcal{W}_2(\mathbb{R})$  denotes the 2-Wasserstein space (see Major [1978], Panaretos and Zemel [2020]). More specifically, we define  $\mathcal{W}_2(\mathbb{R}) = \{F \in \Pi(\mathbb{R})\}$ , where  $\Pi(\mathbb{R})$  is the set of distribution functions over  $\mathbb{R}$  with a finite number of discontinuities.

A natural metric for  $\mathcal{W}_2(\mathbb{R})$  is  $d_{\mathcal{W}_2}^2(F, G)$ , is defined as

$$d_{\mathcal{W}_2}^2(F, G) = \int_0^1 (Q_F(t) - Q_G(t))^2 dt. \quad (3)$$

Here,  $Q_F$  and  $Q_G$  denote the quantile functions of the distribution functions  $F$  and  $G$ , respectively.

Define the discrete-time stochastic process  $Z(\cdot)$  as

$$Z(j) = g(X) + \varepsilon(j), \quad j = 1, \dots, n,$$

where  $X$  is a random vector taking values in  $\mathbb{R}^p$ ,  $g: \mathbb{R}^p \rightarrow \mathbb{R}$  is a continuous function, and for each  $t = 1, \dots, n$ ,  $\varepsilon(t) \sim \mathcal{N}(0, \sigma_\varepsilon^2)$ , with  $\varepsilon(j) \perp \varepsilon(j')$  for  $j \neq j'$ , where  $\perp$  denotes the statistical independence between two random variables, and  $\varepsilon(1), \dots, \varepsilon(n)$  are independent of  $X$ .

Then, we define the element  $F_n \in \mathcal{W}_2(\mathbb{R})$  as

$$F_n(t) = \frac{1}{n} \sum_{j=1}^n \mathbb{I}\{Z(j) \leq t\}. \quad (4)$$

Similarly, we can define the  $\rho$ -th quantile related to  $F_n$  as  $Q_n(\rho) = \inf\{t : F_n(t) \geq \rho\}$ , which has an explicit expression as  $Q_n(\rho) = g(X) + \sum_{j: [j/n] \leq \rho} \varepsilon(j)$ , where  $\varepsilon(j)$  is the  $j$ -th smallest value among  $\{\varepsilon(j)\}_{j=1}^n$ . The expectation of the quantile function can be easily derived as:

$$\mathbb{E}(Q_n(\rho) | X) = g(X) + \sigma_\varepsilon h_n(\rho), \quad (5)$$

where  $h_n(\cdot)$  is a function that depends on the sample size  $n$ .

By the definition of the metric  $d_{\mathcal{W}_2}^2(\cdot, \cdot)$ ,  $[m(X)]^{-1}(\rho) = \mathbb{E}[Q_n(\rho) | X]$ . To see this, we note that

$$m(x) = \operatorname{argmin}_{y \in \mathcal{W}_2(\mathbb{R})} \mathbb{E}(d_{\mathcal{W}_2}^2(F_n, y) | X = x) = \operatorname{argmin}_{y \in \mathcal{W}_2(\mathbb{R})} \mathbb{E} \left( \int_0^1 (Q_n(t) - y^{-1}(t))^2 dt \mid X = x \right) = \mathbb{E}[Q_n | X = x]^{-1}, \quad (6)$$

where, in the final step, we use the property that the mean operator minimizes the square distance in Euclidean space.

Then, the squared Wasserstein distance between the distribution function  $F_n$  with respect to its conditional Fréchet mean  $m(X)$  is calculated as:

$$d_{\mathcal{W}_2}^2(F_n, m(X)) = \int_0^1 \left( g(X) + \sum_{j: [j/n] \leq \rho} \varepsilon(j) - g(X) - \sigma_\varepsilon h_n(\rho) \right)^2 d\rho,$$

which does not depend on the value of  $X$ .

We say that the distribution of  $(X, Y)$  is heteroscedastic with respect to the regression function  $m$  when

$$\mathbb{P}(Y \in \mathcal{B}(m(x), r) | X = x)$$

may depend on  $x$ .

Given a random observation  $X$ , and confidence level  $\alpha \in [0, 1]$ , our goal is to estimate a prediction region  $C^\alpha(X) \subset \mathcal{Y}$  of the response variable  $Y$  that contains the response variable with probability at least  $1 - \alpha$ . First, we introduce the population version of the prediction region.

**Definition 2.** Define the oracle-prediction region as

$$C^\alpha(x) := \mathcal{B}(m(x), r(x)), \quad (7)$$

where  $r(x)$  is the smallest number  $r$  such that  $\mathbb{P}(Y \in \mathcal{B}(m(x), r) | X = x) \geq 1 - \alpha$ .

In this work, we define the prediction region as a ball in the output space, which naturally serves as a level set in a general metric space. We acknowledge that this choice restricts level sets to isotropic regions (with respect to the geometry induced by the metric  $d_2$ ).

In order to estimate  $C^\alpha(x)$ , suppose that we observe a random sample  $\mathcal{D}_n = \{(X_i, Y_i) \in \mathcal{X} \times \mathcal{Y} : i \in [n] := \{1, 2, \dots, n\}\}$  containing independent, identically distributed (i.i.d.) pairs drawn from the same distribution as  $(X, Y)$ . In the rest of this paper, we split  $\mathcal{D}_n$  in two disjoint subsets,  $\mathcal{D}_n = \mathcal{D}_{train} \cup \mathcal{D}_{test}$ , in order to estimate the center and radius of the ball with two independent random samples. We denote the set of indexes  $[S_1] := \{i \in [n] : (X_i, Y_i) \in \mathcal{D}_{train}\}$ ,  $[S_2] := \{i \in [n] : (X_i, Y_i) \in \mathcal{D}_{test}\}$ , and we denote  $|\mathcal{D}_{train}| = n_1$  and  $|\mathcal{D}_{test}| = n_2 = n - n_1$ .

We propose estimators of the oracle-prediction region  $C^\alpha(x)$  of the form  $\tilde{C}^\alpha(x) = \mathcal{B}(\tilde{m}(x), \tilde{r}_\alpha(x))$ , where  $\tilde{m}(x)$  and  $\tilde{r}_\alpha(x)$  are estimators of  $m(x)$  and  $r_\alpha(x)$ . For simplicity, we assume that the outcomes of the estimator  $\tilde{m}(\cdot; \mathcal{D}_{train})$  remain unaffected by the order in which the random elements of  $\mathcal{D}_{train}$  are considered during the estimation process (i.e., the estimator is permutation-invariant). This technical requirement is commonly used in the context of conformal inference.

**Definition 3.** Consider a measurable mapping  $C : \mathcal{X} \rightarrow 2^{\mathcal{Y}}$ . We define the error of  $C$  with respect to the oracle-prediction region as

$$\varepsilon(C, x) = \mathbb{P}(Y \in C(X) \Delta C^\alpha(X) | X = x),$$

where  $C(X) \Delta C^\alpha(X)$  denotes the symmetric difference between the sets  $C(X)$  and  $C^\alpha(X)$ . If  $C = \tilde{C}^\alpha$ , is constructed from  $\mathcal{D}_n$ , then

$$\varepsilon(\tilde{C}, x) = \mathbb{P}(Y \in \tilde{C}^\alpha(X) \Delta C^\alpha(X) | X = x, \mathcal{D}_n).$$

We are interested in the integrated error

$$\mathbb{E}(\varepsilon(\tilde{C}^\alpha, X) | \mathcal{D}_n).$$

We say that  $\tilde{C}^\alpha$  is consistent if

$$\lim_{n \rightarrow \infty} \mathbb{E}(\varepsilon(\tilde{C}^\alpha, X) | \mathcal{D}_n) \rightarrow 0 \text{ in probability.} \quad (8)$$

### 1.3 Contributions

The objective of this paper is to develop a general framework for uncertainty quantification that yields prediction regions for random objects in metric spaces. Now, we summarize and discuss the main contributions of this paper:

1. In the Euclidean setting, the performance and applicability of prediction methods are strongly influenced by the signal-to-noise ratio of the regression model  $m$ . We propose a novel notion of homoscedasticity. Based on this:
2. We propose two uncertainty quantification algorithms, one for the homoscedastic case and another one for the general case.

- (a) Homoscedastic case: We propose a natural generalization of split conformal inference techniques [Vovk et al., 2018, Solari and Djordjilović, 2022] in the context of metric space regression algorithms. We obtain non-asymptotic guarantees of marginal coverage of the type  $\mathbb{P}(Y \in \tilde{C}^\alpha(X)) \geq 1 - \alpha$ . In this setting, we also show that  $\tilde{C}$  is consistent, under mild assumptions, which only require the consistency of the conditional Fréchet mean estimator, i.e.,  $\mathbb{E}(d_2(\tilde{m}(X), m(X)) | \mathcal{D}_{train}) \rightarrow 0$  in probability as  $|\mathcal{D}_{train}| \rightarrow \infty$ . We also establish bounds for the convergence rate of the derived prediction region.
- (b) Heteroscedastic case: We introduce a local  $k$ -nearest neighbor ( $k$ NN) method for predictive inference in metric spaces. Although we do not provide non-asymptotic guarantees for the marginal coverage of the resulting prediction regions, we establish their consistency. Because the algorithm’s performance is highly sensitive to the smoothing parameter  $k$ , we propose a data-driven procedure to select it. The resulting algorithm achieves high statistical efficiency as measured by conditional coverage in both low and high-dimensional response regimes.
- (c) The prediction regions are the generalization of the concept of conditioned quantiles for metric space responses. The prediction regions are defined by a center function  $m$  and a specific radius  $r$  corresponding to a chosen probability level,  $\alpha \in [0, 1]$ . This extension builds upon recent advances in the theory of unconditional quantiles for metric spaces Liu et al. [2022] and provides a natural generalization of the existing concepts.

Arguably, the proposed uncertainty prediction framework built around metric balls offers a more natural construction than existing depth profile methodologies [Zhou and Müller, 2024]. It also extends readily to diverse settings, including causal inference, non-Euclidean predictors, and high-dimensional Euclidean spaces.

Computationally, once the regression function  $m$  is estimated, our uncertainty quantification algorithms can process millions of observations in a few seconds. In contrast, depth-profile methods rely on repeated local polynomial smoothing and can only handle moderate-sized datasets (e.g.,  $n \approx 4,000$ ) within several hours. Consequently, they are ill-suited for big-data scenarios and lack data-driven parameter selection mechanisms for the smoothing parameter  $h$ . Finally, our framework rests on minimal assumptions, whereas depth-profile techniques require the underlying regression estimators to be several times differentiable imposing extra smoothing steps that our method entirely avoids.

3. We evaluate our framework on real-world biomedical datasets, demonstrating its ability to handle complex, high-dimensional non-Euclidean structures. These experiments highlight its suitability for modern digital-health and precision-medicine applications. The different applications involve probability distributions with the 2-Wasserstein metric, fMRI data with graph Laplacians, and multivariate Euclidean data.

## 1.4 General view of existing uncertainty quantification methods

In recent years, uncertainty quantification became an active research area [Geisser, 2017, Politis, 2015]. The impact of uncertainty quantification on data-driven systems has led to a remarkable surge of interest in both applied and theoretical domains. These works address fundamental questions of uncertainty quantification in statistical science and beyond, such as in biomedicine [Hammouri et al., 2023, Banerji et al., 2023].

Geisser’s pioneering book develops a mathematical theory of prediction inference Geisser [2017]. Building upon Geisser’s foundations, Politis presented a comprehensive methodology that effectively applies resampling techniques [Politis, 2015]. Additionally, the book of Vovk, Gammmerman, and Shafer Vovk et al. [2005] (see recent reviews [Angelopoulos and Bates, 2023, Fontana et al., 2023]) has been influential.

One of the most widely used and robust frameworks for quantifying uncertainty in statistical and machine learning models is conformal inference [Shafer and Vovk, 2008]. The central idea of conformal inference is rooted in the concept of exchangeability [Kuchibhotla, 2020]. For simplicity, we assume that the data are independent and identically distributed (i.i.d.). Now, we present a general overview of conformal inference methods for regression models with scalar responses. Consider the sequence  $\mathcal{D}_n = \{(X_i, Y_i)\}_{i=1}^n$  of i.i.d. random variables. Given a new i.i.d. random pair  $(X, Y)$ , conformal prediction, as introduced by Vovk et al. [2005], provides a family of algorithms for constructing prediction intervals independently of the regression algorithm used.

Fix any regression algorithm

$$\mathcal{A} : \cup_{n \geq 0} (\mathcal{X} \times \mathbb{R})^n \rightarrow \{\text{measurable functions } \tilde{m} : \mathcal{X} \rightarrow \mathbb{R}\},$$

which maps a data set containing any number of pairs  $(X_i, Y_i)$ , to a fitted regression function  $\tilde{m}$ . The algorithm  $\mathcal{A}$  is required to treat data points symmetrically, i.e.,

$$\mathcal{A}((x_{\pi(1)}, y_{\pi(1)}), \dots, (x_{\pi(n)}, y_{\pi(n)})) = \mathcal{A}((x_1, y_1), \dots, (x_n, y_n)) \quad (9)$$

for all  $n \geq 1$ , all permutations  $\pi$  on  $[n] = \{1, \dots, n\}$ , and all  $\{(x_i, y_i)\}_{i=1}^n$ . Next, for each  $y \in \mathbb{R}$ , let

$$\tilde{m}^y = \mathcal{A}((X_1, Y_1), \dots, (X_n, Y_n), (X, y))$$

denote the trained model, fitted to the training data together with a hypothesized test point  $(X, y)$ , and let

$$R_i^y = \begin{cases} |Y_i - \tilde{m}^y(X_i)|, & i = 1, \dots, n, \\ |y - \tilde{m}^y(X)|, & i = n + 1. \end{cases} \quad (10)$$

The prediction interval for  $X$  is then defined as

$$\tilde{C}^\alpha(X; \mathcal{D}_n) = \left\{ y \in \mathbb{R} : R_{n+1}^y \leq Q_{1-\alpha} \left( \sum_{i=1}^{n+1} \frac{1}{n+1} \cdot \delta_{R_i^y} \right) \right\}, \quad (11)$$

where  $Q_{1-\alpha} \left( \sum_{i=1}^{n+1} \frac{1}{n+1} \cdot \delta_{R_i^y} \right)$  denotes the quantile of order  $1 - \alpha$  of the empirical distribution  $\sum_{i=1}^{n+1} \frac{1}{n+1} \cdot \delta_{R_i^y}$ .

The full conformal method is known to guarantee distribution-free predictive coverage at the target level  $1 - \alpha$ :

**Theorem 1** (Full conformal prediction). *Vovk et al. [2005] If the data points  $(X_1, Y_1), \dots, (X_n, Y_n), (X, Y)$  are i.i.d. (or more generally, exchangeable), and the algorithm  $\mathcal{A}$  treats the input data points symmetrically as in (9), then the full conformal prediction set defined in (11) satisfies*

$$\mathbb{P}(Y \in \tilde{C}^\alpha(X; \mathcal{D}_n)) \geq 1 - \alpha.$$

A similar result holds for split conformal methods, which involve estimating the regression function on  $\mathcal{D}_{\text{train}}$  and the quantile on  $\mathcal{D}_{\text{test}}$ .

Conformal inference (both split and full) was initially proposed in terms of “nonconformity scores”  $\widehat{S}(X_i, Y_i)$ , where  $\widehat{S}$  is a fitted function that measures the extent to which a data point  $(X_i, Y_i)$  is unusual relative to a training data set  $\mathcal{D}_{train}$ . We have only presented the most commonly used nonconformity score, which is the residual from the fitted model.

$$\widehat{S}(X_i, Y_i) := |Y_i - \widetilde{m}(X_i)|, \quad (12)$$

where  $\widetilde{m}$  is the estimator of the regression function, estimated using random elements from the first split,  $\mathcal{D}_{train}$ .

The non-asymptotic guarantees provided by Theorem 1 can be achieved under more general conditions. For instance, Vovk [2012] established non-asymptotic guarantees with respect to the conditional coverage probability  $\mathcal{D}_n$ , employing the same hypotheses used in Theorem 1. He proves inequalities of the form

$$\mathbb{P}(Y \in \widetilde{C}^\alpha(X; \mathcal{D}_n) \mid \mathcal{D}_n) \geq 1 - \alpha, \quad (13)$$

while Foygel Barber et al. [2021] investigated the case of the probability of conditional coverage with respect to a specific point  $x \in \mathcal{X}$ , which means that

$$\mathbb{P}(Y \in \widetilde{C}^\alpha(X; \mathcal{D}_n) \mid X = x) \geq 1 - \alpha. \quad (14)$$

In the general context of i.i.d. and beyond the conformal inference framework, within the asymptotic regime, Györfi and Walk [2019] presented a kNN-based uncertainty quantification algorithm conditioned on both: i) a random sample  $\mathcal{D}_n$  and ii) covariate characteristics. This algorithm possesses the property that

$$\lim_{n \rightarrow \infty} \mathbb{P}(Y \in \widetilde{C}^\alpha(X; \mathcal{D}_n) \mid \mathcal{D}_n, X = x) = 1 - \alpha \text{ in probability.}$$

The work of Györfi and Walk [2019] is particularly relevant as it provides optimal non-parametric rates for kNN-based uncertainty quantification.

Several authors established non-asymptotic guarantees for the coverage outlined in equation (14). However, in general, this is impossible without incorporating strong assumptions about the joint distribution of  $(X, Y)$  or possessing exact knowledge of the distribution [Foygel Barber et al., 2021, Gibbs et al., 2023].

Lei and Wasserman [2014] show that forcing a prediction algorithm to satisfy the condition in (14) can cause the Lebesgue measure of the estimated prediction region to become unbounded  $\widetilde{C}^\alpha(X; \mathcal{D}_n)$ . More specifically, they prove that it for any continuous probability law  $P$ ,

$$\lim_{n \rightarrow \infty} \mathbb{E}[\text{Leb}(\widetilde{C}^\alpha(X; \mathcal{D}_n))] = \infty,$$

where  $\text{Leb}$  denotes the Lebesgue measure.

**Existing methods for random objects in metric spaces** The only existing uncertainty quantification algorithm with a comparable goal is the conformal approach proposed by Zhou and Müller [2024]. Their procedure constructs prediction regions for responses that reside in a general metric space, but it is limited to scalar predictors (or, in the multivariate setting, to a single-index projection step). The method relies on a two-stage local polynomial estimation of conditional distribution functionals, and its precision is sensitive to the bandwidth parameter  $h$ . As a result, it does not extend smoothly to non-Euclidean predictors, non-differentiable models, or high-dimensional covariate spaces. Algorithm 1 outlines the core steps the algorithm of

[Zhou and Müller, 2024].

---

**Algorithm 1** Conformal prediction for random responses in metric spaces and scalar predictors [Zhou and Müller, 2024]

---

**Require:** Confidence level  $\alpha \in (0, 1)$ , kernel  $K_h$ , split fraction  $\tau \in (0, 1)$ .

- 1: **Data split.** Randomly split  $\mathcal{D}_n = \{(X_i, Y_i)\}_{i=1}^n \subset \mathbb{R} \times \mathcal{Y}$  into training set  $\mathcal{D}_{\text{train}}$  of size  $\lfloor \tau n \rfloor$  and calibration set  $\mathcal{D}_{\text{test}}$ .
- 2: **Conditional distance profiles.** For each  $x \in \mathcal{X}$  and  $\omega \in Y$ , estimate

$$\tilde{F}_{\omega, x}(t) = \frac{\sum_{i \in \mathcal{D}_{\text{train}}} K_h(x - X_i) \mathbf{1}\{d(\omega, Y_i) \leq t\}}{\sum_{i \in \mathcal{D}_{\text{train}}} K_h(x - X_i)}, \quad t \geq 0.$$

- 3: **Average transport cost.**

$$\tilde{C}(\omega | x) = \int_0^\infty |\tilde{F}_{\omega, x}(t) - \hat{F}_{Y, x}(t)| dt.$$

- 4: **Conditional profile score.**

$$\tilde{S}(z | x) = \frac{\sum_{i \in \mathcal{D}_{\text{train}}} K_h(x - X_i) \mathbf{1}\{\tilde{C}(Y_i | X_i) \leq z\}}{\sum_{i \in \mathcal{D}_{\text{train}}} K_h(x - X_i)}, \quad z \geq 0.$$

- 5: **Calibration quantile.** For each  $(X_i, Y_i) \in \mathcal{D}_{\text{test}}$ , set  $\tilde{S}_i := \tilde{S}(\tilde{C}(Y_i | X_i) | X_i)$  and define

$$\tilde{Q}_{1-\alpha} = \text{Quantile}_{(1-\alpha)\left(1 + \frac{1}{|\mathcal{D}_{\text{cal}}|}\right)} \{\tilde{S}_i : i \in \mathcal{D}_{\text{test}}\}.$$

- 6: **Scoring a new covariate.** For a new random predictor  $X_{n+1} \in \mathbb{R}$  and any  $y \in \mathcal{Y}$ , compute  $\tilde{C}(y | X_{n+1})$  and  $\tilde{S}(\tilde{C}(y | X_{n+1}) | X_{n+1})$ .
- 7: **Prediction set.**

$$\tilde{C}_\alpha(X_{n+1}) = \{y \in \mathcal{Y} : \tilde{S}(\tilde{C}(y | X_{n+1}) | X_{n+1}) \leq \tilde{Q}_{1-\alpha}\}.$$


---

## 2 Mathematical models

In this section, we present a framework for uncertainty quantification, based on the previous definition of the oracle prediction region (see Section 1.2):

$$C^\alpha(x) := \mathcal{B}(m(x), r(x)). \quad (15)$$

Recall that  $r(x)$  is the smallest number  $r$  such that  $\mathbb{P}(Y \in \mathcal{B}(m(x), r) | X = x) \geq 1 - \alpha$ .

The initial phase of our uncertainty quantification methodology entails the estimation of the Fréchet regression function  $m : \mathcal{X} \rightarrow \mathcal{Y}$ .

In the second step, we determine the radius that governs the number of points contained within the prediction regions. This selection is made to ensure that the set includes at least  $(1 - \alpha)$  proportion of points from the dataset.

We emphasize that our method establishes, for different confidence levels  $\alpha \in [0, 1]$ , different level sets for the prediction regions problem. This approach allows us to associate the prediction regions with the notion of conditional quantiles for metric space responses, generalizing the

marginal approaches from Liu et al. [2022].

## 2.1 Homoscedastic case

Algorithm 2 outlines the core steps of our uncertainty quantification method for the homoscedastic case. The algorithm estimates the function  $m$  and the radius  $r$  by dividing the data into two independent datasets.

In the homoscedastic case, the distribution of  $d_2(Y, m(x))$  remains invariant regardless of the point  $x \in \mathcal{X}$ . As a result, it is natural to estimate the radius using the empirical distribution of the random sample  $\mathcal{D}_{test} = \{d_2(Y_i, \tilde{m}(X_i))\}_{i \in [S_2]}$ . Then, we can formulate a conformalized version of this algorithm to attain non-asymptotic guarantees of the form  $\mathbb{P}(Y \in \tilde{C}^\alpha(X; \mathcal{D}_n)) \geq 1 - \alpha$ . The idea of estimating different quantities of the model in different splits is not new in the literature on conformal inference. This approach increases the computational feasibility of the methods, providing non-asymptotic guarantees and facilitating theoretical asymptotic analysis. However, there may be some loss in statistical efficiency due to estimating model quantities in different subsamples. These methods, known as split conformal methods, have been extensively studied (see, for example, Vovk et al. [2018], Solari and Djordjilović [2022]).

---

### Algorithm 2 Uncertainty quantification algorithm; homoscedastic case

---

1. Estimate the function  $m(\cdot)$ , by  $\tilde{m}(\cdot)$  using the random sample  $\mathcal{D}_{train}$ .
  2. For all  $i \in [S_2]$ , evaluate  $\tilde{m}(X_i)$  and define  $\tilde{r}_i = d_2(Y_i, \tilde{m}(X_i))$ .
  3. Estimate the empirical distribution  $\tilde{G}^*(t) = \frac{1}{n_2} \sum_{i \in [S_2]} \mathbb{I}\{\tilde{r}_i \leq t\}$  and denote by  $\tilde{q}_{1-\alpha}$  the empirical quantile of level  $1 - \alpha$  of the empirical distribution function  $\tilde{G}^*(t)$ .
  4. Return  $\tilde{C}^\alpha(x; \mathcal{D}_n) = \mathcal{B}(\tilde{m}(x), \tilde{q}_{1-\alpha})$ .
- 

We have the following marginal finite sample guarantee:

**Proposition 2.** *For any estimator  $\tilde{m}$ , assuming the random elements  $\{(X_i, Y_i)\}_{i=1}^n$  are i.i.d. with respect to a pair  $(X, Y)$ , Algorithm 2 satisfies:*

$$\mathbb{P}(Y \in \tilde{C}^\alpha(X; \mathcal{D}_n)) \geq 1 - \alpha.$$

*Proof.* This follows by observing that

$$\begin{aligned} \mathbb{P}(Y \in \tilde{C}^\alpha(X; \mathcal{D}_n)) &= \mathbb{P}(Y \in \mathcal{B}(\tilde{m}(X), \tilde{q}_{1-\alpha})) \\ &= \mathbb{E}[\mathbb{I}\{d_2(Y, \tilde{m}(X)) \leq \tilde{q}_{1-\alpha}\}] \geq 1 - \alpha. \end{aligned}$$

□

**Remark 2.** *Proposition 2 holds in both in homoscedastic and heteroscedastic cases. However, when we apply Algorithm 2 to a heteroscedastic model, the resulting conditional coverage can substantially deviate from the true value. Under such circumstances, the algorithm may not be consistent.*

**Remark 3.** *In Algorithm 2, when handling discrete spaces, it becomes crucial to incorporate randomization strategies in the radius estimation. This ensures that for any two distinct  $\tilde{r}_j$  and  $\tilde{r}_{j'}$ , the probability of them being equal is precisely zero (with probability one).*

This general strategy has been extensively explored, including Kuchibhotla [2020] (see Definition 1), and Cauchois et al. [2021], which specifically focuses on discrete structures. The integration of randomization techniques in such scenarios leads to:

$$1 - \alpha + \frac{1}{n_2 + 1} \geq \mathbb{P}(Y \in \tilde{C}^\alpha(X; \mathcal{D}_n)) \geq 1 - \alpha.$$

### 2.1.1 Statistical consistency

Next we introduce the technical assumptions that ensure the asymptotic consistency of Algorithm 2.

**Assumption 1.** Suppose that the following hold:

1.  $n_2 \rightarrow \infty$ .
2.  $\tilde{m}$  is a consistent estimator in the sense that  $\lim_{n_1 \rightarrow \infty} \mathbb{E}(d_2(\tilde{m}(X), m(X)) | \mathcal{D}_{train}) \rightarrow 0$ , in probability.
3. The population quantile  $q_{1-\alpha} = \inf\{t \in \mathbb{R} : G(t) = \mathbb{P}(d_2(Y, m(X)) \leq t) = 1 - \alpha\}$  is unique and is a continuity point of the function  $G(\cdot)$ .

**Theorem 3.** Under Assumption 1, the estimated prediction region  $\tilde{C}^\alpha(x; \mathcal{D}_n)$  obtained using Algorithm 2 satisfies

$$\lim_{n \rightarrow \infty} \mathbb{E}(\varepsilon(\tilde{C}^\alpha(X; \mathcal{D}_n))) \rightarrow 0 \text{ in probability.} \quad (16)$$

*Proof.* See Appendix. □

**Assumption 2.** Suppose that for all  $t \in \mathbb{R}$ , the distribution function of distances  $G(t, x) = \mathbb{P}(d_2(Y, m(x)) \leq t | X = x)$  is uniformly Lipschitz with constant  $L$  in the sense that for all  $t, t' \in \mathbb{R}$  and for all  $x \in \mathcal{X}$ , we have  $|G(t, x) - G(t', x)| \leq L|t - t'|$ .

**Example 3.** Suppose that  $\mathcal{X} = \mathbb{R}^p$ ,  $\mathcal{Y} = \mathbb{R}^m$ ,  $d_1(\cdot, \cdot) = d_2(\cdot, \cdot) = \|\cdot - \cdot\|$  ( $L^2$  norm), and consider the regression model

$$Y = m(X) + \varepsilon, \quad (17)$$

where  $\varepsilon$  is a random vector taking values in  $\mathbb{R}^m$ , and independent from  $X$ . Let  $f$  be the density function of the random variable  $\varepsilon$ . If the density function  $f$  is bounded, then,  $G$  is uniformly Lipschitz.

**Remark 4.** Suppose that the assumptions of Example 3 are satisfied. Consider any estimator  $\tilde{m}$  of  $m$ , and define the distribution of the distances:

$$G^*(t, x) = \mathbb{P}(d_2(Y, \tilde{m}(X)) \leq t | X = x).$$

We can express this probability in terms of the perturbation introduced by the estimator:

$$G^*(t, x) = \mathbb{P}(\|\varepsilon + (m(X) - \tilde{m}(X))\| \leq t | X = x).$$

Then for all  $x$ , the function  $G^*(t, x)$  is Lipschitz continuous.

We now provide a non-asymptotic bound on the expected coverage error of both the estimated prediction region and the oracle prediction region. Intuitively, this error can be controlled by the estimation errors of the regression function  $m$  and of the calibration quantile  $q_{1-\alpha}$ .

**Proposition 4.** *Under Assumptions 1 and 2, and assuming that  $G^*(t, x) = \mathbb{P}(d_2(Y, \tilde{m}(X)) \leq t \mid X = x)$ , is uniformly Lipschitz, we have:*

$$\mathbb{E}(\varepsilon(\tilde{C}^\alpha, X) \mid \mathcal{D}_n) \leq C(\mathbb{E}(d_2(\tilde{m}(X), m(X)) \mid \mathcal{D}_{train}) + 4(|\tilde{q}_{1-\alpha} - q_{1-\alpha}|)),$$

where  $C$  is a positive constant depending on the Lipschitz constants of the functions  $G$  and  $G^*$ .

*Proof.* See Appendix. □

**Example 4.** *Suppose that  $\mathcal{X} = \mathbb{R}^p$ ,  $\mathcal{Y} = \mathbb{R}^m$ , and  $d_1(\cdot, \cdot) = d_2(\cdot, \cdot) = \|\cdot - \cdot\|$  (the  $L^2$  norm). Consider the regression model*

$$Y = m(X) + \varepsilon, \tag{18}$$

where  $\varepsilon$  is a random vector taking values in  $\mathbb{R}^m$  and is independent of  $X$ . Let  $f$  denote the density function of  $\varepsilon$ . For, this model Proposition 4 implies

$$\mathbb{E}(\varepsilon(\tilde{C}^\alpha, X) \mid \mathcal{D}_n) \leq C(\mathbb{E}(d_2(\tilde{m}(X), m(X)) \mid \mathcal{D}_{train}) + 4(|\tilde{q}_{1-\alpha} - q_{1-\alpha}|)).$$

**Remark 5.** *In the absence of covariates and assuming the Fréchet mean  $m$  is known, the estimation rate depends solely on the convergence speed of the quantile estimator for pseudo-residuals*

$$r = d(Y, m(X)).$$

*In this homoscedastic setting, our bounds extend the optimality results of Györfi and Walk [2019] for the univariate empirical distribution, yielding a rate of  $O(\sqrt{\ln n/n})$ . When  $m$  is unknown but can be estimated, at the parametric rate  $O(n^{-1/2})$ , our algorithm can achieve fast convergence rates. For an explicit model-specific rate calculation, one must account for the error in estimating  $m$  and propagate it into the quantile estimation for  $q_{1-\alpha}$ . To do this, one can invoke measurement-error quantile-estimation results from Hansmann and Kohler [2017].*

**Remark 6.** *More specific non-asymptotic results can be derived for homoscedastic cases and univariate responses, as demonstrated in Corollary 1 of Foygel Barber et al. [2021]. In their work, the authors impose more stringent assumptions to bound the Lebesgue measure, including requirements such as the existence of a density function for the random error  $\varepsilon$  and symmetrical conditions, alongside stability criteria for the underlying mean regression functions  $m$ . In our setting, we construct the level set using balls without imposing any smoothness assumptions. We only assume the integrated asymptotic consistency of the regression function  $m$ .*

## 2.2 Heteroscedastic case

The homoscedastic assumption can be too restrictive in metric spaces that lack a linear structure, making a local approach more appropriate. In this paper, we adopt the  $k$ -nearest neighbors (kNN) regression algorithm Fix and Hodges [1951], Biau and Devroye [2015] for this purpose, as it is both computationally efficient and easy to implement.

In heteroscedastic methods, given a point  $x \in \mathcal{X}$ , we repeat the same steps as in the homoscedastic algorithm, but the radius estimation only considers data points in a neighborhood of  $x$ , denoted as  $N_k(x) = \{i \in [S_2] : d_2(X_i, x) \leq d_{2(n_2, k)}(x)\}$ . Here,  $d_{2(n_2, k)}(x)$  represents the distance between  $x$  and its  $k$ -th nearest neighbor in the test dataset  $\mathcal{D}_{test}$  using the distance  $d_2$ . Algorithm 3 provides a full detailed outline of this procedure.

---

**Algorithm 3** Uncertainty quantification algorithm; for heteroscedastic case

---

1. Estimate the function  $\tilde{m}(\cdot)$  using the random sample  $\mathcal{D}_{\text{train}}$ .
  2. For a given point  $x \in \mathcal{X}$ , let  $X_{(n_2,1)}(x), X_{(n_2,2)}(x), \dots, X_{(n_2,k)}(x)$  denote the  $k$ -nearest neighbors of  $x$  in increasing order based on the distance  $d_2$ . For each data point  $X_i$  in  $\mathcal{D}_{\text{test}}$ , compute the predicted value  $\tilde{m}(X_i)$ . Then, define the residual  $\tilde{r}_i$  as the distance between the response value  $Y_i$  and the predicted value  $\tilde{m}(X_i)$ , i.e.,  $\tilde{r}_i = d_2(Y_i, \tilde{m}(X_i))$ . Denote the residuals associated with the  $i$ -th ordered observation as  $\tilde{r}_{(n_2,i)}(x) = d_2(Y_{(n_2,i)}, \tilde{m}(x))$ .
  3. Estimate the empirical distribution of conditional distribution by  $\tilde{G}_k^*(x, t) = \frac{1}{k} \sum_{i=1}^k \mathbb{I}\{\tilde{r}_{(n_2,i)}(x) \leq t\}$  and denote by  $\tilde{q}_{1-\alpha}(x)$  the empirical quantile of level  $1 - \alpha$  of the empirical distribution  $\tilde{G}_k^*(x, t)$ .
  4. Return the estimated prediction region as  $\tilde{C}^\alpha(x) := \tilde{C}^{\alpha,k}(x) = \mathcal{B}(\tilde{m}(x), \tilde{q}_{1-\alpha}(x))$ .
- 

**Remark 7.** Although Algorithm 3 can be consistent, finite sample-guarantees are not easy to prove. To address this limitation and propose a heteroscedastic algorithm with non-asymptotic performance guarantees, we suggest extending the conformal quantile methodology introduced by Romano et al. [2019] to our context. Specifically, we aim to achieve  $\mathbb{P}(Y \in \tilde{C}^\alpha(X; \mathcal{D}_n)) \geq 1 - \alpha$ . The core steps are outlined below:

1. **Estimation of  $m(\cdot)$ :** Utilize the dataset  $\mathcal{D}_{\text{train}}$  to estimate the regression function  $m(\cdot)$ .
2. **Estimation of  $r(\cdot)$ :** Employ the random sample  $\mathcal{D}_{\text{test}}$  and the pairs  $(X_i, d_2(Y_i, \tilde{m}(X_i)))$  for each  $i \in [S_2]$  to estimate the radius function  $r(\cdot)$ .
3. **Calibration of  $\tilde{r}(x)$ :** In an additional data set  $\mathcal{D}_{\text{test}2}$ , we calibrate the radius  $\tilde{r}(x)$  to obtain non-asymptotic guarantees using the scores  $S_i = d_2(Y_i, \tilde{m}(X_i)) - \tilde{r}(X_i)$ . The empirical quantile at level  $\alpha$ , denoted by  $\tilde{w}_\alpha$ , is then used to define the final radius function as  $\hat{r}(x) = \tilde{r}(x) + \tilde{w}_\alpha$ .

### 2.2.1 Statistical Theory

The following technical assumptions are introduced to guarantee that the proposed heteroscedastic  $k$ NN-algorithm is asymptotically consistent.

**Assumption 3.** 1.  $n_1, n_2 \rightarrow \infty$ .

2.  $\tilde{m}$  is a consistent estimator in the sense that  $\mathbb{E}(d_2(\tilde{m}(X), m(X)) | \mathcal{D}_{\text{train}}) \rightarrow 0$  in probability as  $n_1 \rightarrow \infty$ .
3. As  $n_2 \rightarrow \infty$ ,  $k \rightarrow \infty$ , and  $\frac{k}{n_2} \rightarrow 0$ .
4. Except in a set of probability zero, for all  $x \in \mathcal{X}$ , the pointwise population quantile  $q_{1-\alpha}(x) = \inf\{t \in \mathbb{R} : G(t, x) = \mathbb{P}(d_2(Y, m(x)) \leq t | X = x) = 1 - \alpha\}$  exists uniquely and is a continuity point of the function  $G(\cdot, x)$ .
5. Except in a set of probability zero, for all  $x \in \mathcal{X}$ ,  $\mathbb{E}(d_2(Y, m(x)) | X = x) < \infty$ .

**Theorem 5.** Under Assumption 3, the uncertainty quantification estimator  $\tilde{C}^\alpha(\cdot)$  obtained using Algorithm 3 satisfies:

$$\lim_{n \rightarrow \infty} \mathbb{E}(\varepsilon(\tilde{C}^\alpha, X) | \mathcal{D}_n) \rightarrow 0.$$

*Proof.* The proof is given in the Appendix. □

**Remark 8.** We can generalize Proposition 4 using Assumption 3 for the  $k$ NN algorithm (and introducing another modified Lipschitz condition for the radius estimation  $r = d_2(Y, m(X))$ , see Györfi and Walk [2019]):

$$\mathbb{E}(\varepsilon(\tilde{C}^\alpha, X) | \mathcal{D}_n) \leq C(\mathbb{E}(d_2(\tilde{m}(X), m(X)) | \mathcal{D}_{train}) + 4(\mathbb{E}(|\tilde{q}_{1-\alpha}(X) - q_{1-\alpha}(X)|))).$$

In the heteroscedastic case, we must consider explicitly the impact of the conditional quantile  $q_{1-\alpha}(x)$  for each  $x \in \mathcal{X}$  in the rate. In a similar context, Györfi and Walk [2019] propose the optimal rate for prediction intervals, which coincides when the conditional regression function  $m$  is known and is given by  $O\left(\frac{\ln n}{n^{p+2}}\right)$  for  $p \geq 1$ , where  $p$  denotes the dimension of the predictor  $X$ . It is important to note that this rate scales with the dimension of the covariate space  $p$ , unlike in the homoscedastic case.

### 2.3 Optimized $k$ NN algorithm with parameter selection

From a practical standpoint, the original  $k$ NN heteroscedastic algorithm is highly sensitive to the tuning parameter used for radius estimation. To mitigate this, Algorithm 4 adopts a fully  $k$ NN-based predictive inference procedure that selects the value of  $k$  via data splitting: we choose  $k$  to optimize both the Fréchet mean estimator and the marginal coverage on an independent validation sample. For the Fréchet mean, we use leave-one-out cross validation following Azadkia [2020] in order to select the parameter  $k$  for the regression function  $m$ , which provides theoretical guarantees in finite dimensional Euclidean spaces. Although this approach is not designed to yield non-asymptotic coverage guarantees and may not align perfectly with marginal calibration, we nonetheless optimize the coverage criterion when estimating the prediction radius. Given the data-adaptive nature of the algorithm, we expect this strategy to improve overall model performance and achieve competitive properties in non-asymptotic conditional coverage validity.

### 2.4 Regression algorithms in metric spaces: Random Forest, Global Fréchet regression method, and $k$ NN

In this section, we introduce a general background on regression modeling in metric spaces needed to implement our predictive algorithms in practice. We first introduce two nonparametric regression alternatives:  $k$ NN and Random Forests. Finally, we introduce the global Fréchet regression algorithm as a parametric model for metric spaces outcomes.

Before proceeding, recall that the target  $m$  is the conditional Fréchet mean

$$m(x) = \arg \min_{y \in \mathcal{Y}} \mathbb{E}[d_1^2(Y, y) | X = x],$$

whose estimation must be made feasible in practice.

**$k$ NN estimator.** Given an i.i.d. sample  $\mathcal{D}_n = \{(X_i, Y_i)\}_{i=1}^n \subset \mathcal{X} \times \mathcal{Y}$ , the naive yet effective estimator calculates the Fréchet mean locally

---

**Algorithm 4** Tuning  $k$ NN uncertainty quantification algorithm in metric spaces; heteroscedastic case

---

**Stage 1: Local selection of optimal bandwidth via Fréchet mean**

1. Estimate the regression function  $\tilde{m}(\cdot)$  using the training sample  $\mathcal{D}_{\text{train}}$  as follows. For each point  $x \in \mathcal{D}_{\text{train}}$ , and each candidate  $k \in \mathcal{K}_{\text{grid}}$  ( $\mathcal{K}_{\text{grid}}$  is a list of potential  $k$ -values), define the  $k$ -nearest neighbors  $\mathcal{N}_k^{\text{LOO}}(x)$  excluding  $x$ , and compute:

$$E_k(x) = \frac{1}{k} \sum_{j \in \mathcal{N}_k^{\text{LOO}}(x)} d_1(Y_j, \tilde{m}(x))$$

2. For each  $x \in \mathcal{D}_{\text{test}}$ , select the locally optimal bandwidth:

$$k_{\text{Fréchet}}^*(x) = \arg \min_{k \in \mathcal{K}_{\text{grid}}} E_k(x)$$

**Stage 2: Global selection via marginal coverage calibration**

1. For each candidate  $k \in \mathcal{K}_{\text{grid}}$ , and each  $x \in \mathcal{D}_{\text{test}}$ , compute pseudo-residuals  $\tilde{r}_i = d_2(Y_i, \tilde{m}(X_i))$ , then estimate:

$$Q_{1-\alpha}(x; k) = \text{quantile}_{1-\alpha} \left( \{\tilde{r}_j\}_{j \in \mathcal{N}_k(x)} \right)$$

2. Construct the prediction region  $\tilde{C}^{\alpha, k}(x) = \mathcal{B}(\tilde{m}(x), \tilde{q}_{1-\alpha}(x; k))$ , and evaluate marginal coverage:

$$\widetilde{\text{Coverage}}(k) = \frac{1}{|\mathcal{D}_{\text{test}}|} \sum_{(X_i, Y_i) \in \mathcal{D}_{\text{test}}} \mathbb{I} \{ Y_i \in \tilde{C}^{\alpha, k}(X_i) \}$$

3. Select the global optimal  $k_{\text{marg}}^* = \arg \min_{k \in \mathcal{K}_{\text{grid}}} \left| \widetilde{\text{Coverage}}(k) - (1 - \alpha) \right|$
4. For a point  $x \in \mathcal{X}$ , define the final prediction region:

$$\tilde{C}^{\alpha}(x) = \mathcal{B}(\tilde{m}(x), \tilde{q}_{1-\alpha}(x; k_{\text{marg}}^*))$$


---

$$\tilde{m}_k(x) = \arg \min_{y \in \mathcal{Y}} \frac{1}{k} \sum_{i \in N_k(x)} d_1^2(Y_i, y),$$

where  $N_k(x)$  denotes the indices of the  $k$  nearest neighbors of the point  $x$  in the training sample  $\mathcal{D}_{\text{train}}$ , with respect to a distance  $d_1$  that measure the similarity of the elements in the predictor space. A generalization of this algorithm to non-Euclidean predictor spaces, based on the concept of  $k$ -prototypes, was proposed by Cohen and Kontorovich [2022]. The authors established the universal consistency of the estimator under mild regularity conditions—conditions that are also satisfied by our uncertainty quantification algorithms.

**Random Forest regressogram estimator.** Recently, a Random Forest for non-Euclidean predictors and responses was introduced by Capitaine et al. [2024]. Let  $\pi_n$  denote a partitioning

rule that can be estimated for the specific split tree rules introduced in [Capitaine et al., 2024]. The corresponding Fréchet regressogram estimator is

$$\tilde{m}(x) = \arg \min_{y \in \mathcal{Y}} \frac{1}{n} \sum_{i=1}^n d_1^2(Y_i, y) \mathbb{I}\{X_i \in \pi_n[x]\},$$

where  $\pi_n[x]$  is the unique cell containing  $x$ . Over this tree–algorithm, the authors define a random forest algorithm.

Under the regularity conditions specified by Capitaine et al. for universal consistency, our prediction region algorithm is consistent. However, these theoretical guarantees require that the metric space have a finite diameter and that the associated regression functions  $m$  satisfy smoothing (differentiability) assumptions that are not imposed by the  $k$ NN based approach of Cohen and Kontorovich [2022].

**Global Fréchet Algorithm** Now, we focus on a specific parametric and less flexible regression model designed for outcomes valued in the metric space, known as *global Fréchet regression model* [Petersen and Müller, 2019].

The global Fréchet regression model provides a natural extension of the standard linear regression model from Euclidean spaces to metric spaces.

In particular, Petersen and Müller [2019] propose to model the regression function in the form

$$m(x) = \operatorname{argmin}_{y \in \mathbb{R}} \mathbb{E} [\omega(x, X) d^2(Y, y)] ,$$

where the weight function  $\omega$  is defined by

$$\omega(x, z) = 1 + (z - \mu)^\top \Sigma^{-1} (x - \mu)$$

with  $\mu = \mathbb{E}(X)$  and  $\Sigma = \operatorname{Cov}(X)$ . As Petersen and Müller [2019] show, in the case of  $\mathcal{Y} = \mathcal{H}$ , where  $\mathcal{H}$  is a separable Hilbert space with an inner product  $\langle \cdot, \cdot \rangle$ , this model reduces to standard linear regression.

While in our applications we primarily focus on developing estimators in the global Fréchet regression model, it is important to emphasize that our uncertainty quantification algorithm can be applied to any regression technique, including random forests in metric spaces. It should be noted, however, that if the global Fréchet models do not align with the conditional Fréchet mean  $m$ , the resulting estimators will be inconsistent.

To estimate the conditional mean function  $m(x)$  under the global Fréchet model from a random sample  $\mathcal{D}_n = \{(X_i, Y_i)\}_{i=1}^n$ , we may solve the counterpart empirical problem

$$\tilde{m}(x) = \operatorname{argmin}_{y \in \mathcal{Y}} \frac{1}{n} \sum_{i=1}^n [\omega_{in}(x) d_1^2(y, Y_i)], \quad (19)$$

where  $\omega_{in}(x) = \left[ 1 + (X_i - \bar{X}) \tilde{\Sigma}^{-1} (x - \bar{X}) \right]$ , with  $\bar{X} = \frac{1}{n} \sum_{i=1}^n X_i$ , and  $\tilde{\Sigma} = \frac{1}{n-1} \sum_{i=1}^n (X_i - \bar{X})(X_i - \bar{X})^\top$ .

### 3 Simulation Study

We conducted a simulation study to evaluate the empirical performance of the proposed uncertainty quantification framework. The goal is twofold: i) Evaluate the conditional coverage performance of our methods, compared to state–of–the–art methods both in scalar and in metric–space settings (see [Zhou and Müller, 2024]); ii) examine the degradation of  $k$ NN algorithm’s

performance as the ambient dimension of the random response increases, considering both homoscedastic and heteroscedastic designs. Additional simulations about marginal coverage for different data structures are presented in the Supplemental Material.

### 3.1 Conditional Coverage Examination

Most state-of-the-art conformal methods are designed primarily for scalar responses. Moreover, reliable estimation of conditional coverage is generally feasible only in low-dimensional settings and is interpretable when predictors and responses are scalar. For these reasons, our initial comparison of conditional coverage performance focuses on scalar-to-scalar regression, although we also evaluate the existing metric-space approach [Zhou and Müller, 2024]. Unlike the simulation scenarios proposed in Zhou and Müller [2024], where the generative models are quasi-deterministic, our scenarios feature high noise levels.

Here, we focus on the conditional coverage

$$\mathbb{P}\left(Y \in \tilde{C}^\alpha(X) \mid X\right),$$

achieved by the optimized heteroscedastic  $k$ NN predictive procedure (see Section 2.3 for further details).

We focus on comparisons using established Euclidean space conformal methods: the HPD-split scores of Izbicki et al. [2022] (denoted as HPD1 and HPD2 in the result tables) and several variants of Conformalized Quantile Regression (CQR) [Romano et al., 2019]. The HPD-split implementation uses the `dist` and `hpd` functions from <https://github.com/rizbicki/predictionBands>, while CQR is evaluated under the default settings of the `cfSurvival` package. For completeness, we also benchmark against the method of Zhou and Müller [2024], the only competitor specifically designed for metric space responses.

For each scenario, we generate  $B = 100$  independent datasets of size  $n = 2000$ , which we reserve for evaluating conditional coverage. We estimate conditional coverage by fitting a generalized additive model (GAM) to approximate the population quantity

$$p^\alpha(x) = \mathbb{P}(\mathbb{I}\{Y \in C^\alpha(x)\} = 1 \mid X = x).$$

For each replicate  $b \in \{1, \dots, B\}$ , we measure the deviation from the nominal level  $\alpha$  via the  $L^2$  error:

$$\widehat{\text{Err}}_b^\alpha = \int_0^5 \{\widehat{p}^\alpha(x) - (1 - \alpha)\}^2 dx,$$

and we report the average error across all replicates:

$$\frac{1}{B} \sum_{b=1}^B \widehat{\text{Err}}_b^\alpha.$$

**Simulation Settings** In our simulation study, we generate data from four scalar to scalar models that encompass linear, nonlinear, homoscedastic, and heteroscedastic structures. Our method employs a  $k$ NN based heteroscedastic predictive model, using optimized selection strategies for Fréchet mean estimation and radius estimation step.

**Setting 1 (Linear, heteroscedastic).**

$$X \sim \mathcal{U}(0, 5), \quad \varepsilon \sim \mathcal{U}(-1, 1), \quad Y = 3 + X + X\varepsilon.$$

**Setting 2 (Non-linear, heteroscedastic; uniform noise).**

$$X \sim \mathcal{U}(0, 5), \quad \varepsilon \sim \mathcal{U}(-1, 1), \quad Y = 3 + e^X + X \varepsilon.$$

**Setting 3 (Non-linear, heteroscedastic; Gaussian noise).**

$$X \sim \mathcal{U}(0, 5), \quad \varepsilon \sim \mathcal{N}(0, 4), \quad Y = 3 + e^X + X \varepsilon.$$

**Setting 4 (Additive, homoscedastic).**

$$X, \varepsilon \sim \mathcal{U}(0, 5), \quad Y = X + \varepsilon.$$

**Results** Table 1 summarizes the mean  $L^2$  prediction errors for  $\alpha \in \{0.20, 0.10, 0.05\}$  and sample sizes  $n \in \{1000, 3000\}$ . Our method computes prediction sets in a few seconds, whereas the depth profile approaches (implemented in C++) require approximately 30 minutes when  $n = 3000$ . Across the four simulation settings, our procedure achieves the smallest conditional coverage error, with particularly marked improvements in the nonlinear scenarios (Settings 2 and 3). In Settings 1 and 4, some scalar–response methods can slightly outperform ours, but the differences are negligible, and those alternatives deteriorate quickly in the heteroscedastic scenarios. Competing metric space approaches are highly sensitive to the noise levels considered here, likely because they must sequentially estimate multiple nonparametric model components.

Table 1:  $L^2$  integrated error for the conditional coverage for the four generative examples considered.

| Method               | $\alpha = 0.20$ |                | $\alpha = 0.10$ |                | $\alpha = 0.05$ |                |
|----------------------|-----------------|----------------|-----------------|----------------|-----------------|----------------|
|                      | $n = 1000$      | $n = 3000$     | $n = 1000$      | $n = 3000$     | $n = 1000$      | $n = 3000$     |
| <b>Scenario 1</b>    |                 |                |                 |                |                 |                |
| <b>Our Method #1</b> | <b>0.04850</b>  | <b>0.04490</b> | <b>0.05260</b>  | <b>0.05040</b> | <b>0.03190</b>  | <b>0.03090</b> |
| Metric-Profile       | 0.14310         | 0.14060        | 0.13840         | 0.13570        | 0.09010         | 0.08790        |
| Conformal Quantile   | 0.05020         | 0.04850        | 0.03750         | 0.03520        | 0.01750         | 0.01680        |
| HPD-1                | 0.15860         | 0.15920        | 0.08910         | 0.08960        | 0.02360         | 0.02580        |
| HPD-2                | 0.21610         | 0.22010        | 0.10480         | 0.10480        | 0.04520         | 0.04840        |
| <b>Scenario 2</b>    |                 |                |                 |                |                 |                |
| <b>Our Method #1</b> | <b>0.11419</b>  | <b>0.11239</b> | <b>0.04591</b>  | <b>0.04153</b> | <b>0.02499</b>  | <b>0.02328</b> |
| Metric-Profile       | 0.37777         | 0.37956        | 0.29009         | 0.28932        | 0.17272         | 0.16677        |
| Conformal Quantile   | 0.45365         | 0.45346        | 0.34097         | 0.33808        | 0.17876         | 0.17677        |
| HPD-1                | 0.21786         | 0.21548        | 0.10058         | 0.09910        | 0.02946         | 0.03006        |
| HPD-2                | 0.22241         | 0.22385        | 0.10399         | 0.10511        | 0.04995         | 0.05000        |
| <b>Scenario 3</b>    |                 |                |                 |                |                 |                |
| <b>Our Method #1</b> | <b>0.09905</b>  | <b>0.09279</b> | <b>0.06206</b>  | <b>0.06164</b> | <b>0.03306</b>  | <b>0.03186</b> |
| Metric-Profile       | 0.30556         | 0.30794        | 0.26213         | 0.26478        | 0.15654         | 0.16383        |
| Conformal Quantile   | 0.35631         | 0.35565        | 0.28209         | 0.28361        | 0.12431         | 0.12915        |
| HPD-1                | 0.21485         | 0.21074        | 0.16653         | 0.15640        | 0.03055         | 0.02972        |
| HPD-2                | 0.24625         | 0.24548        | 0.18966         | 0.17730        | 0.04256         | 0.04299        |
| <b>Scenario 4</b>    |                 |                |                 |                |                 |                |
| <b>Our Method #1</b> | <b>0.02981</b>  | <b>0.02622</b> | <b>0.02006</b>  | <b>0.02005</b> | <b>0.02370</b>  | <b>0.02516</b> |
| Metric-Profile       | 0.04654         | 0.04495        | 0.11655         | 0.11388        | 0.09042         | 0.09093        |
| Conformal Quantile   | 0.02107         | 0.01942        | 0.02150         | 0.01927        | 0.01322         | 0.01333        |
| HPD-1                | 0.05265         | 0.05374        | 0.02556         | 0.02692        | 0.01223         | 0.01001        |
| HPD-2                | 0.04653         | 0.04780        | 0.02861         | 0.02936        | 0.01429         | 0.01339        |

### 3.2 Effects of Dimension: Homoscedastic vs. Heteroscedastic Algorithms

We now focus on estimating the impact of the response dimension  $p$  of the outcome  $Y$  on the statistical efficiency of conditional coverage.

Consider the generative model

$$Y | X = x \sim \mathcal{N}_p(\mu(x)\mathbf{1}_p, \sigma^2(x)\mathbf{I}_p), \quad \mu(x) = 5 + \sum_{j=1}^d x_j, \quad X \sim \text{Unif}[0, 1]^d,$$

where  $\sigma^2 : \mathbb{R}^d \rightarrow \mathbb{R}$  denotes the variance function. We study two signal–noise regimes: *Homoscedastic case*:  $\sigma(x) = 1$  for all  $x \in [0, 1]^d$ ; *Heteroscedastic case*:  $\sigma(x) = 4 + \sum_{j=1}^d x_j$ .

The *oracle* global prediction region at level  $1 - \alpha$ , understood as the minimum volume band, is

$$C^\alpha(x) = \prod_{s=1}^p \left[ \mu(x) \pm \sigma(x) \sqrt{\chi_{p,1-\alpha}^2} \right].$$

We apply both the  $k$ NN homoscedastic algorithm and the  $k$ NN heteroscedastic conformal procedure (with optimal parameter selection) for response dimensions  $p \in \{1, 50, 100\}$  and sample size  $n = 5000$ , fixing the predictor dimension to  $d = 1$ . In this way, we can accurately estimate conditional coverage while keeping the computations tractable.

Conditional coverage is estimated through a generalized additive model (GAM):

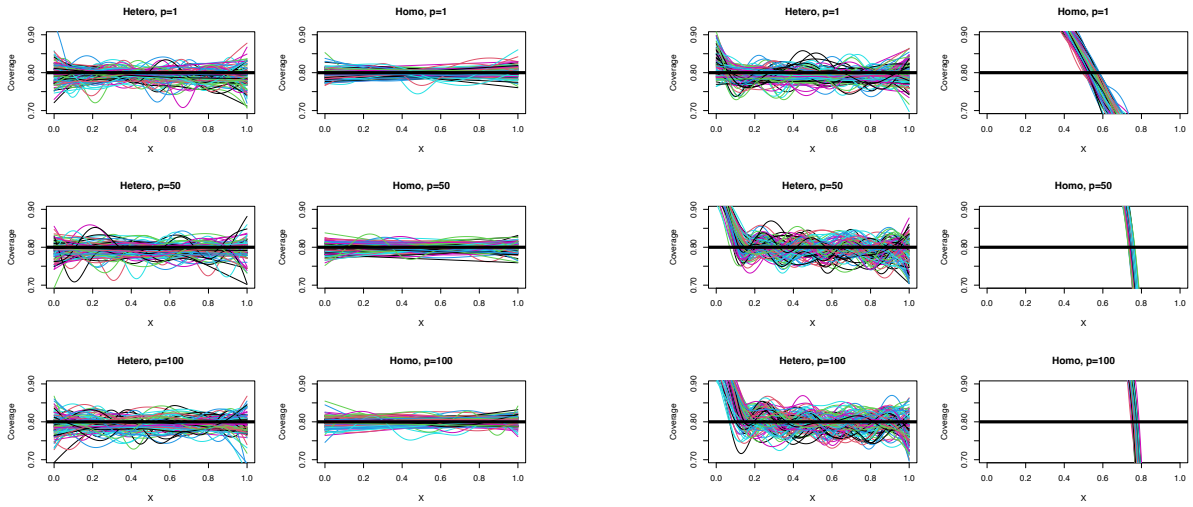
$$p^\alpha(x) = \mathbb{P}(\mathbb{I}\{Y \in C^\alpha(x)\} = 1 | X = x).$$

Figures 1 and 2 display results over 100 simulations for different values of  $X$  and response dimensions  $p$ , at  $\alpha = 0.2$  and  $\alpha = 0.05$ , respectively, in both signal–to–noise regimes. As expected, the homoscedastic algorithm is robust and invariant to  $X$  in the homoscedastic regime. Conversely, when applied there, the heteroscedastic model remains stable but is less accurate than the homoscedastic algorithm, consistent with intuition.

In the heteroscedastic regime, the homoscedastic algorithm exhibits poor conditional calibration: although its marginal coverage is close to the nominal level, its conditional coverage may deviate significantly. (In fact, it falls outside the range  $(0.7, 0.9)$  over part of the domain of  $X$ ). For the heteroscedastic algorithm, performance deteriorates as the response dimension  $p$  increases, especially for small values of  $X$  ( $X < 0.2$ ). Across both algorithms with high-dimensional responses, conditional coverage errors reach up to 0.05 or higher, indicating the general difficulty of accurately approximating conditional coverage in heteroscedastic settings. Finally, since both methods rely on  $k$ NN based nonparametric approximations, they require increasing amounts of data as  $p$  grows. In practice, if the true signal-to-noise relationship is homoscedastic, one should choose the homoscedastic algorithm to guarantee more robust results in high-dimensional settings. We note that we have only one predictor; with multiple predictors, the advantages of the homoscedastic algorithm in this setup would be even greater.

## 4 Analysis of real-world clinical data

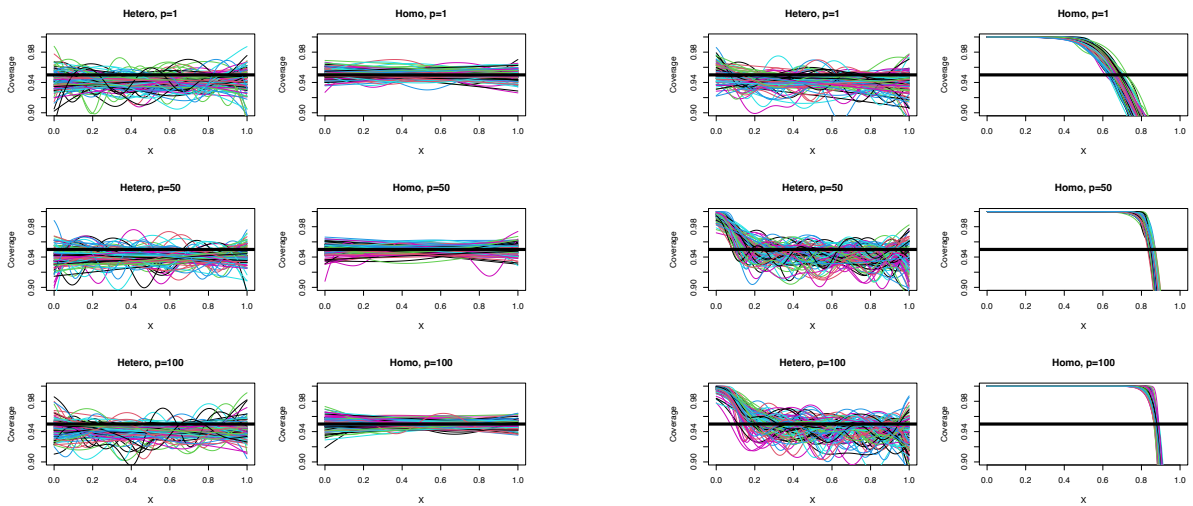
In this section, we illustrate the general applicability of our algorithm to diverse data structures using real-world clinical datasets. First, we apply shape analysis to characterize the progression of Parkinson’s disease via handwritten digital biomarkers in the absence of covariates. Next, for each remaining example, we assume independent observations  $(X, Y) \in \mathcal{X} \times \mathcal{Y}$  and employ an appropriate regression algorithm to estimate the regression function  $m$ . Additional results for



(a) Signal–Noise homoscedastic

(b) Signal–Noise heteroscedastic

Figure 1: Conditional coverage trajectories for  $\alpha = 0.2$  and  $B = 100$  simulations.



(a) Signal–Noise Homocedastic

(b) Signal–Noise heteroscedastic

Figure 2: Conditional coverage trajectories for  $\alpha = 0.05$  and  $B = 100$  simulations.

other data structures are provided in the Supplemental Material.

## 4.1 Shape Analysis

### 4.1.1 Motivation

Shape analysis is a research area that demands novel statistical methods in metric spaces (e.g., Dryden and Mardia, 2016; Steyer et al., 2023) and finds broad applications in the biomedical sciences. This framework is especially powerful for modeling random objects through their geometric features. In this study, we focus on the shapes of handwritten samples drawn from patients with a neurological disorder and compare them to those from a control group of healthy individuals. Our goal in this section is to construct prediction regions—at a chosen confidence level  $\alpha \in (0, 1)$ —that capture the typical handwriting trajectories of healthy subjects. We posit that an individuals with the neurological disorder will produce writing shapes that fall outside these regions. By doing so, we can both flag individuals whose trajectories deviate substantially from the control distribution and characterize their atypical behaviors as outliers.

### 4.1.2 Data Description

This study employs data from Isenkul et al. [2014], comprising  $n_1 = 15$  control subjects and  $n_2 = 30$  individuals diagnosed with Parkinson’s disease, to analyze handwriting shapes captured through digital tests. Our objective is to establish expected predictions regions at different confidence levels  $\alpha$  based on the control group’s data. For this purpose, first we estimate the empirical Fréchet mean using Euclidean distance  $d_1^2(\cdot, \cdot) = \|\cdot - \cdot\|^2$ . Subsequently, we adopt  $d_2(\cdot, \cdot) = \|\cdot - \cdot\|_\infty$  to graphically represent the tolerance regions for various individuals across confidence levels, utilizing the convex hull of extreme points for visualization purposes.

### 4.1.3 Results

Figure 3 shows handwriting trajectories overlaid with tolerance regions at confidence levels  $\alpha = 0.5$  and  $\alpha = 0.3$ , highlighting those from individuals with Parkinson’s disease in yellow. Using the  $\alpha = 0.5$  region, we correctly classify more than 75% of Parkinson’s patients by checking whether their trajectories lie outside the healthy control region. These results underscore the promise of our uncertainty quantification framework for validating novel digital biomarkers as the case of handwriting shapes in clinical applications.

## 4.2 Multidimensional Euclidean data

### 4.2.1 Motivation

Multivariate Euclidean response data, is increasingly prevalent in clinical outcome analysis, particularly in the integration of multiple biomarkers to enhance diagnostic accuracy for various diseases. This approach is exemplified in diabetes research, where at least two biomarkers - Fasting Plasma Glucose (FPG) and Glycosylated Hemoglobin (A1C) - are considered in the diagnosis of the disease. In this simple 2–dimensional example, providing naive uncertainty quantification measures is far from trivial due to the lack of a natural order in  $\mathbb{R}^2$ . Moreover, bivariate quantile estimation methods can depend on a specific notion of order tailored to each problem, as discussed in Klein and Kneib [2020].

This section aims to illustrate our uncertainty quantification framework, which can accommodate any distance  $d_2$  to define the prediction region  $C^\alpha(\cdot)$ , and overcome technical difficulties associated with defining a multivariate quantile. We consider the standard Euclidean distance

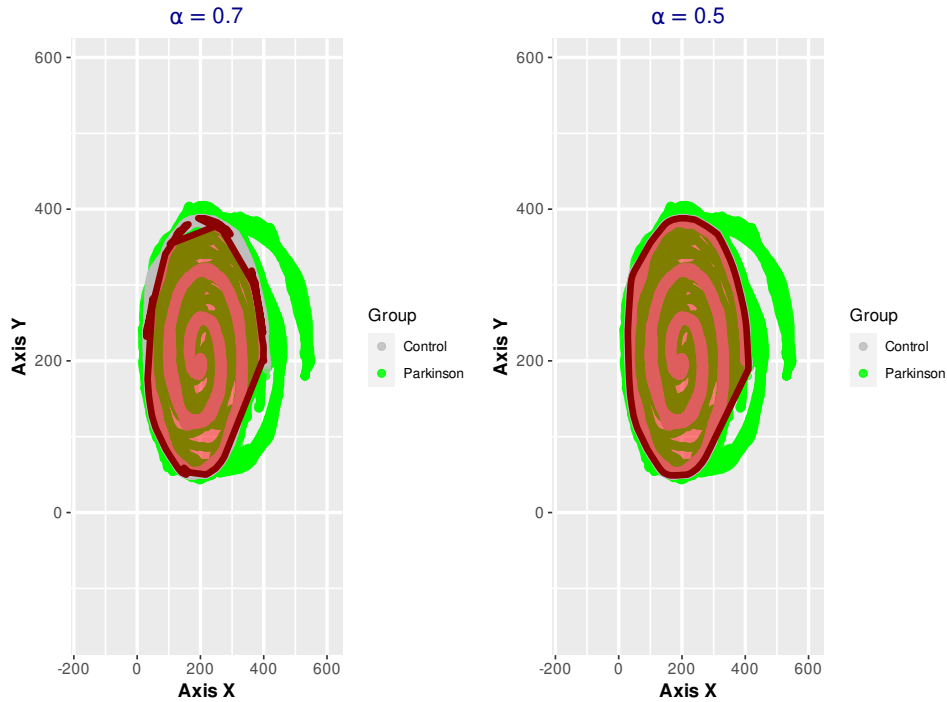


Figure 3: Tolerance regions in expectations for various confidence levels in the written test using control individuals as a reference. The plots depict the raw trajectories of both control and Parkinson’s patients. We do not introduce covariates in the derivation of prediction regions for the Fréchet mean.

$d_2^2(x, y) = \sum_{i=1}^m (x_i - y_i)^2$  for all  $x, y \in \mathbb{R}^m$ . Continuing with the discussion on diabetes, we focus on a scientific application in this field.

To demonstrate the application of our methodology, we consider the mentioned biomarkers: FPG and A1C as a response of the regression models that in this case will be a multivariate-response linear model. The goal is to create predictive models to estimate the continuous outcomes used to diagnose and monitor the progression of diabetes mellitus.

Uncertainty analysis is crucial in clinical prediction models, as it helps understand the advantages and disadvantages of these models. In cases where there is significant uncertainty in the regression model, it may be necessary to construct a more complex model incorporating new patient characteristic attributes. Alternatively, considering more sophisticated regression models, such as neural networks, might enhance the predictive capacity of the models.

#### 4.2.2 Data Description

We conducted an extensive study using a comprehensive dataset from the National Health and Nutrition Examination Survey (NHANES) cohort (see more details Matabuena et al. [2023a]), comprising a substantial number of individuals ( $n = 58,972$ ). For our analysis, we utilized predictor and response variables described in Table 2, and applied a linear multivariate regression model to estimate the function  $m$ . We considered  $k = 200$  as the number of neighbors in the kNN method.

Our study aimed to address two primary objectives: firstly, to demonstrate the remarkable computational efficiency of our algorithm, and secondly, to underscore the importance of quantifying uncertainty in standard disease risk scores. In an ideal clinical context, the primary clinical goal is to establish a simple and cost-effective risk score that could accurately capture

patients’ glucose conditions without relying on traditional diabetes diagnostic variables, and stratify the risk of diabetes to promote new public health interventions Matabuena et al. [2024]. With uncertainty quantification, we can evaluate whether our regression model  $m$  can be useful for such clinical purposes.

### 4.2.3 Results

The implementation of our algorithm in the NHANES dataset exhibited remarkable efficiency, with execution times of just a few seconds.

Figure 4 presents the results to apply the uncertainty quantification region in three patients. We observe individual uncertainty differences when we predict the A1C and FPG biomarkers based on individual clinical characteristics. Patient (C), characterized as young and healthy (see Table 2), is predicted to be in the non-diabetes range with low uncertainty. In contrast, patient (A), who is older, has a high waist circumference, and elevated systolic pressure, is predicted to fall within the diabetes and prediabetes range, despite exhibiting glucose profiles characteristic of a non-diabetic healthy individual. These outcomes underscore the need for more sophisticated variables to accurately predict the true glycemic patient status, as also evidenced by the marginal  $R^2$  for each variable that takes values equal to 0.12 and 0.08, respectively for the A1C and FPG. In Matabuena et al. [2024], we provide evidence that incorporation of at least one diabetes biomarker that directly measures the glucose of individuals, such as FPG or A1C, for building reliable predictive models. Essentially, this highlights that predicting Diabetes Mellitus is impossible without considering specific glucose measurements or proxy variables for them.

| ID        | Age | Waist  | Systolic Pressure | Diastolic Pressure | Triglycerides | Glucose | Glycosylated Hemoglobin |
|-----------|-----|--------|-------------------|--------------------|---------------|---------|-------------------------|
| 45424 (A) | 76  | 114.30 | 144               | 66                 | 64            | 91.00   | 5.10                    |
| 31858 (B) | 55  | 107.70 | 128               | 70                 | 72            | 98.00   | 7.60                    |
| 28159 (C) | 23  | 84.60  | 124               | 64                 | 147           | 81.00   | 5.40                    |

Table 2: Characteristics of three patients in a real-life example where the response variable is multivariate (bivariate) Euclidean data.

## 4.3 Distributional Representation of Biosensor Time Series

### 4.3.1 Motivation

The field of distributional data analysis has seen significant growth [Klein, 2023, Matabuena et al., 2022a, Meunier et al., 2022], largely due to its critical role in understanding the marginal distributional characteristics of biological time series in regression modeling. We investigate the probability distributions within continuous glucose monitor (CGM) time series data [Matabuena et al., 2021a], vital for discerning distributional patterns like hypoglycemia, and hyperglycemia in diabetes research. Figure 5 illustrates such transformation in the case of a one non-diabetic and diabetic individual

We focus on analyzing biological outcomes defined in the space  $\mathcal{Y} = \mathcal{W}_2(T)$ , comprising univariate continuous probability distributions supported  $T = [40, 400] \subset \mathbb{R}$ . This work emphasizes "distributional representation" through quantile functions, aiming to enrich our understanding of glucose profiles’ impacts from various factors beyond CGM simple summary as CGM mean and - standard deviation values estimated with the raw glucose time series.

Given a random sample of healthy individuals, the goal of our analysis is to provide the reference quantile glucose values with our uncertainty quantification algorithm across different age groups.

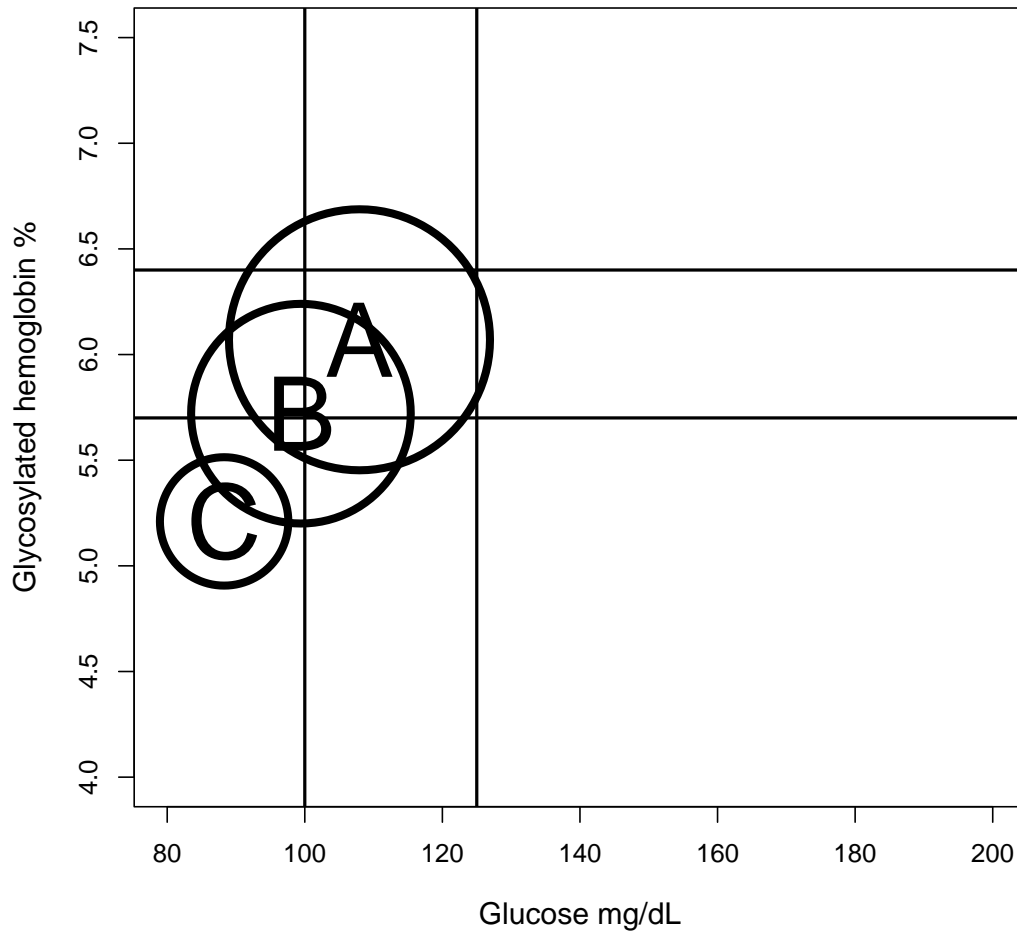


Figure 4: Prediction regions for three patients based on the geometry of the Euclidean distance. The black lines in the plot indicate the transition between prediabetes and diabetes status. Patient (C) is normoglycemic, while the other two patients, (A) and (B), exhibit oscillations between two glyceimic statuses. Patient (B) is characterized as normoglycemic and diabetic, while patient A shows diabetes and prediabetes. The plot highlights the varying glyceimic patterns according to patient characteristics.

The determination of this reference profile can have various applications, such as detecting individuals at high risk of diabetes mellitus, as well as determining threshold criteria considering the latest advancements about glucose homeostasis provided by a CGM monitor. We note that the glucose values at least, in average glucose levels increase with the age, and according to this biological behaviour, we must move to a medicine based on personalized criteria. The use of CGM one distributional representations allows to examine this biological phenomenon in all, low, middle and high-glucose concentrations.

### 4.3.2 Data Description

Data from Shah et al. [2019], which collected glucose values at 5-minute intervals over several days from non-diabetic individuals in everyday settings, was considered in our analysis. This

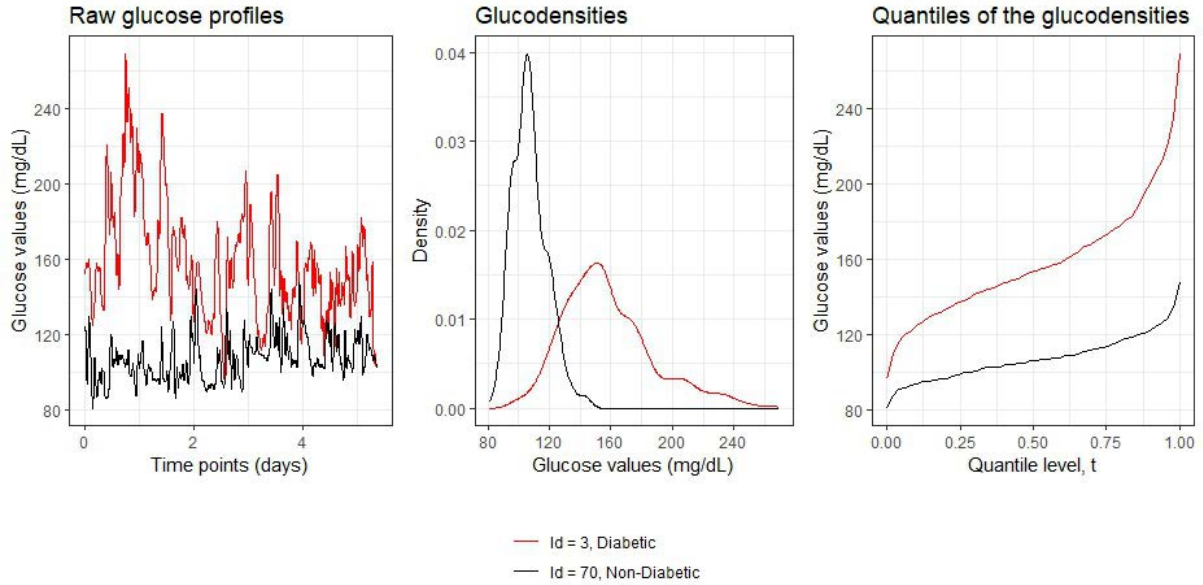


Figure 5: The figure presents the process of transformation CGM time series of two individuals in their marginal density functions and marginal quantile functions.

data was originally collected to establish normative glucose ranges with simple summaries as CGM mean values by age. Extending this foundation, we adopt the distributional perspective of CGM data as our regression model's response, utilizing the 2-Wasserstein distance (equivalently, quantile representation) in Global Fréchet regression. For analysis and visualization, we apply the distance  $d_2(\cdot, \cdot) = \|\cdot - \cdot\|_\infty$ , setting the confidence level at  $\alpha = 0.2$  and the kNN smoothing parameter to  $k = 30$ .

### 4.3.3 Results

The application of our uncertainty quantification algorithm shows a variation in uncertainty levels across different age groups, as outlined in Figure 6. However, the analysis reveals a consistent conditional mean of glucose across ages but a marked increase in the uncertainty of quantile glucose values with the increase of the age of patients. These clinical findings enhance our capability to classify and monitor health in non-diabetics through CGM. This approach to defining disease states offers a pathway towards personalized medicine, as evidenced by its application in our research on personalized sarcopenia definitions Matabuena et al. [2023a], where the response variable was finite-dimensional outcome ( $\mathcal{Y} = \mathbb{R}^2$ ).

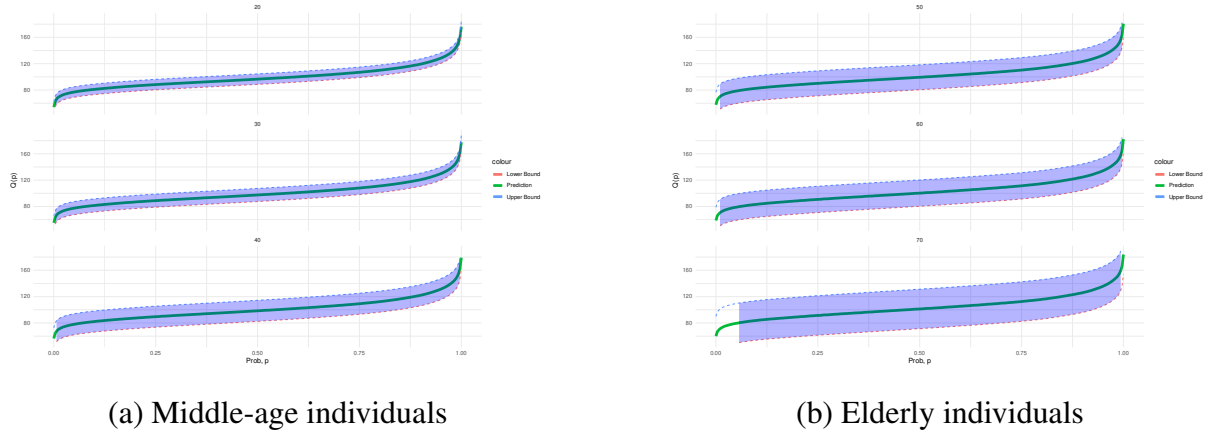


Figure 6: The figure presents the normative continuous glucose monitoring (CGM) distributional values across different age groups, with a confidence level  $\alpha = 0.2$ . Our analysis indicates that while the conditional mean values remain similar across different age groups, there is an increase in uncertainty as age increases.

## 5 Discussion

This paper introduces a framework for deriving prediction regions in regression models on metric spaces. In the homoscedastic case, our approach generalizes split conformal methods by employing a conformal score based on the distance between random response elements and their Fréchet mean. For the heteroscedastic setting, inspired by [Györfi and Walk, 2019], we develop two novel algorithms based on  $kNN$  to construct prediction regions in metric space regression. Through extensive simulations and theoretical analysis, we demonstrate the effectiveness of our methods in various data analysis scenarios. We show that our assumptions are weaker than those of [Zhou and Müller, 2024], and that our estimator admits explicit guarantees of the convergence rates. Moreover, it is computationally scalable and, when paired with appropriate tuning parameters, outperforms the other methods in several simulation studies.

In the heteroscedastic setting, we select model parameters via an adaptive, data-driven splitting criterion. In future work, we plan to extend our methods to causal inference problems Bhattacharjee et al. [2025] such as synthetic controls Kurisu et al. [2025] as well as other scientific questions involving dependent data.

## Acknowledgments

The authors are grateful to Ruoyu Wang for providing constructive feedback on the manuscript. This research was partially supported by US Horizon 2020 research and innovation program under grant agreement No. 952215 (TAILOR Connectivity Fund). Gábor Lugosi acknowledges the support of Ayudas Fundación BBVA a Proyectos de Investigación Científica 2021 and the Spanish Ministry of Economy and Competitiveness, Grant PGC2018-101643-B-I00 and FEDER, EU.

## References

Anastasios N. Angelopoulos and Stephen Bates. Conformal prediction: A gentle introduction. *Foundations and Trends® in Machine Learning*, 16(4):494–591, 2023. ISSN 1935-8237. doi: 10.1561/2200000101. URL <http://dx.doi.org/10.1561/2200000101>.

- Mona Azadkia. Optimal choice of  $k$  for  $k$ -nearest neighbor regression, 2020. URL <https://arxiv.org/abs/1909.05495>.
- Christopher R. S. Banerji, Tapabrata Chakraborti, Chris Harbron, and Ben D. MacArthur. Clinical ai tools must convey predictive uncertainty for each individual patient. *Nature Medicine*, Oct 2023. ISSN 1546-170X. doi: 10.1038/s41591-023-02562-7. URL <https://doi.org/10.1038/s41591-023-02562-7>.
- Rina Foygel Barber, Emmanuel J. Candès, Aaditya Ramdas, and Ryan J. Tibshirani. Conformal prediction beyond exchangeability. *The Annals of Statistics*, 51(2):816 – 845, 2023. doi: 10.1214/23-AOS2276. URL <https://doi.org/10.1214/23-AOS2276>.
- Stephen Bates, Emmanuel Candès, Lihua Lei, Yaniv Romano, and Matteo Sesia. Testing for outliers with conformal p-values. *The Annals of Statistics*, 51(1):149–178, 2023.
- Satarupa Bhattacharjee and Hans-Georg Müller. Single index fréchet regression. *arXiv preprint arXiv:2108.05437*, 2021. doi: 10.48550/ARXIV.2108.05437. URL <https://arxiv.org/abs/2108.05437>.
- Satarupa Bhattacharjee and Hans-Georg Müller. Geodesic mixed effects models for repeatedly observed/longitudinal random objects. *arXiv preprint arXiv:2307.05726*, 2023.
- Satarupa Bhattacharjee, Bing Li, and Lingzhou Xue. Nonlinear global fréchet regression for random objects via weak conditional expectation. *arXiv preprint arXiv:2310.07817*, 2023.
- Satarupa Bhattacharjee, Bing Li, Xiao Wu, and Lingzhou Xue. Doubly robust estimation of causal effects for random object outcomes with continuous treatments, 2025. URL <https://arxiv.org/abs/2506.22754>.
- Gérard Biau and Luc Devroye. *Lectures on the nearest neighbor method*, volume 246. Springer, 2015.
- Matthieu Bulté and Helle Sørensen. Medoid splits for efficient random forests in metric spaces. *arXiv preprint arXiv:2306.17031*, 2023.
- Emmanuel Candès, Lihua Lei, and Zhimei Ren. Conformalized survival analysis. *Journal of the Royal Statistical Society Series B: Statistical Methodology*, 85(1):24–45, 01 2023. ISSN 1369-7412. doi: 10.1093/jrsssb/qkac004. URL <https://doi.org/10.1093/jrsssb/qkac004>.
- Louis Capitaine, Jérémie Bigot, Rodolphe Thiébaud, and Robin Genuer. Fréchet random forests for metric space valued regression with non euclidean predictors. *Journal of Machine Learning Research*, 25(355):1–41, 2024.
- Maxime Cauchois, Suyash Gupta, and John C Duchi. Knowing what you know: valid and validated confidence sets in multiclass and multilabel prediction. *Journal of Machine Learning Research*, 22(81):1–42, 2021.
- Han Chen and Hans-Georg Müller. Sliced wasserstein regression. *arXiv preprint arXiv:2306.10601*, 2023.

- Yaqing Chen, Zhenhua Lin, and Hans-Georg Müller. Wasserstein regression. *Journal of the American Statistical Association*, 116(535):1–14, 2021. doi: 10.1080/01621459.2021.1956937. URL <https://doi.org/10.1080/01621459.2021.1956937>.
- Jiayi Cheng and Peilin Yang. Conformal inference for heterogeneous policy effect. 2022.
- Victor Chernozhukov, Kaspar Wüthrich, and Yinchu Zhu. Distributional conformal prediction. *Proceedings of the National Academy of Sciences*, 118(48):e2107794118, 2021a.
- Victor Chernozhukov, Kaspar Wüthrich, and Yinchu Zhu. An exact and robust conformal inference method for counterfactual and synthetic controls. *Journal of the American Statistical Association*, 116(536):1849–1864, 2021b.
- Raj S Chhikara and Irwin Guttman. Prediction limits for the inverse gaussian distribution. *Technometrics*, 24(4):319–324, 1982.
- Dan Tsir Cohen and Aryeh Kontorovich. Metric-valued regression. *ArXiv Preprint*, 2022.
- Srinjoy Das, Yiwen Zhang, and Dimitris N Politis. Model-based and model-free point prediction algorithms for locally stationary random fields. *arXiv preprint arXiv:2212.03079*, 2022.
- Thomas G Dietterich and Jesse Hostetler. Conformal prediction intervals for markov decision process trajectories. *arXiv preprint arXiv:2206.04860*, 2022.
- Tom Dietterich and Jesse Hostetler. Reinforcement learning prediction intervals with guaranteed fidelity. *arXiv preprint*, 2025.
- Jacopo Diquigiovanni, Matteo Fontana, and Simone Vantini. Conformal prediction bands for multivariate functional data. *Journal of Multivariate Analysis*, 189:104879, 2022.
- Ian L Dryden and Kanti V Mardia. *Statistical shape analysis: with applications in R*, volume 995. John Wiley & Sons, 2016.
- Paromita Dubey and Hans-Georg Müller. Fréchet analysis of variance for random objects. *Biometrika*, 106(4):803–821, 2019.
- Paromita Dubey and Hans-Georg Müller. Modeling time-varying random objects and dynamic networks. *Journal of the American Statistical Association*, 117(540):2252–2267, 2022. doi: 10.1080/01621459.2021.1917416. URL <https://doi.org/10.1080/01621459.2021.1917416>.
- Paromita Dubey, Yaqing Chen, and Hans-Georg Müller. Depth profiles and the geometric exploration of random objects through optimal transport. *arXiv preprint arXiv:2202.06117*, 2022.
- Robin Dunn, Larry Wasserman, and Aaditya Ramdas. Distribution-free prediction sets for two-layer hierarchical models. *Journal of the American Statistical Association*, pages 1–12, 2022.
- Jianing Fan and Hans-Georg Müller. Conditional Wasserstein barycenters and interpolation/extrapolation of distributions. *arXiv preprint arXiv:2107.09218*, 2021.
- E Fix and JL Hodges. Discriminatory analysis, nonparametric discrimination usa school of medicine. *Texas: Rendolph Field*, 1952, 1951.

- Edwin Fong and Chris C Holmes. Conformal bayesian computation. *Advances in Neural Information Processing Systems*, 34:18268–18279, 2021.
- Matteo Fontana, Gianluca Zeni, and Simone Vantini. Conformal prediction: a unified review of theory and new challenges. *Bernoulli*, 29(1):1–23, 2023.
- Alex Fout and Bailey K Fosdick. Fréchet covariance and manova tests for random objects in multiple metric spaces. *arXiv preprint arXiv:2306.12066*, 2023.
- Rina Foygel Barber, Emmanuel J Candès, Aaditya Ramdas, and Ryan J Tibshirani. The limits of distribution-free conditional predictive inference. *Information and Inference: A Journal of the IMA*, 10(2):455–482, 2021.
- Donald AS Fraser and Irwin Guttman. Tolerance regions. *The Annals of Mathematical Statistics*, 27(1):162–179, 1956.
- Maurice René Fréchet. Les éléments aléatoires de nature quelconque dans un espace distancié. *Annales de l’institut Henri Poincaré*, 10(4):215–310, 1948. URL [http://www.numdam.org/item/AIHP\\_1948\\_\\_10\\_4\\_215\\_0](http://www.numdam.org/item/AIHP_1948__10_4_215_0).
- Alexander Gammernan, Vovk Vladimir, and Vladimir Vapnik. Learning by transduction. In *Proceedings of the 1st Annual Conference on Uncertainty in Artificial Intelligence (UAI-85)*, pages 148–155, 1998.
- Carlos García-Meixide and Marcos Matabuena. Causal survival embeddings: non-parametric counterfactual inference under censoring. *arXiv preprint arXiv:2306.11704*, 2023.
- Jakob Gawlikowski, Cedrique Rovile Njietcheu Tassi, Mohsin Ali, Jongseok Lee, Matthias Humt, Jianxiang Feng, Anna Kruspe, Rudolph Triebel, Peter Jung, Ribana Roscher, et al. A survey of uncertainty in deep neural networks. *Artificial Intelligence Review*, pages 1–77, 2023.
- Gery Geenens, Alicia Nieto-Reyes, and Giacomo Francisci. Statistical depth in abstract metric spaces. *Statistics and Computing*, 33(2):46, Feb 2023. ISSN 1573-1375. doi: 10.1007/s11222-023-10216-4. URL <https://doi.org/10.1007/s11222-023-10216-4>.
- Seymour Geisser. *Predictive inference*. Chapman and Hall/CRC, 2017.
- Aritra Ghosal, Marcos Matabuena, Wendy Meiring, and Alexander Petersen. Predicting distributional profiles of physical activity in the nhanes database using a partially linear single-index fréchet regression model. *arXiv preprint arXiv:2302.07692*, 2023.
- Rahul Ghosal and Marcos Matabuena. Multivariate scalar on multidimensional distribution regression, 2023.
- Rahul Ghosal, Vijay R Varma, Dmitri Volfson, Inbar Hillel, Jacek Urbanek, Jeffrey M Hausdorff, Amber Watts, and Vadim Zipunnikov. Distributional data analysis via quantile functions and its application to modelling digital biomarkers of gait in Alzheimer’s disease. *Biostatistics*, 11 2021a. ISSN 1465-4644. doi: 10.1093/biostatistics/kxab041. URL <https://doi.org/10.1093/biostatistics/kxab041>. kxab041.

- Rahul Ghosal, Vijay R Varma, Dmitri Volfson, Jacek Urbanek, Jeffrey M Hausdorff, Amber Watts, and Vadim Zipunnikov. Scalar on time-by-distribution regression and its application for modelling associations between daily-living physical activity and cognitive functions in alzheimer’s disease. *arXiv preprint arXiv:2106.03979*, 2021b.
- Isaac Gibbs, John J Cherian, and Emmanuel J Candès. Conformal prediction with conditional guarantees. *arXiv preprint arXiv:2305.12616*, 2023.
- L Györfi and Harro Walk. Nearest neighbor based conformal prediction. In *Annales de l’ISUP*, volume 63, pages 173–190, 2019.
- Michael Hamada, Valen Johnson, Leslie M Moore, and Joanne Wendelberger. Bayesian prediction intervals and their relationship to tolerance intervals. *Technometrics*, 46(4):452–459, 2004.
- Ziad Akram Ali Hammouri, Pablo Rodríguez Mier, Paulo Félix, Mohammad Ali Mansournia, Fernando Huelin, Martí Casals, and Marcos Matabuena. Uncertainty quantification in medicine science: The next big step. *Archivos de Bronconeumología*, 2023. ISSN 0300-2896. doi: <https://doi.org/10.1016/j.arbres.2023.07.018>. URL <https://www.sciencedirect.com/science/article/pii/S0300289623002338>.
- Steve Hanneke. Universally consistent online learning with arbitrarily dependent responses. In *International Conference on Algorithmic Learning Theory*, pages 488–497. PMLR, 2022.
- Matthias Hansmann and Michael Kohler. Estimation of quantiles from data with additional measurement errors. *Statistica Sinica*, pages 1661–1673, 2017.
- Xiaoyu Hu and Jing Lei. A two-sample conditional distribution test using conformal prediction and weighted rank sum. *Journal of the American Statistical Association*, pages 1–19, 2023.
- Muhammed Isenkul, Betül Sakar, Olcay Kursun, et al. Improved spiral test using digitized graphics tablet for monitoring parkinson’s disease. In *The 2nd international conference on e-health and telemedicine (ICEHTM-2014)*, volume 5, pages 171–175, 2014.
- Rafael Izbicki, Gilson Shimizu, and Rafael B Stern. Cd-split and hpd-split: Efficient conformal regions in high dimensions. *Journal of Machine Learning Research*, 23(87):1–32, 2022.
- Jeong Min Jeon, Young Kyung Lee, Enno Mammen, and Byeong U. Park. Locally polynomial Hilbertian additive regression. *Bernoulli*, 28(3):2034 – 2066, 2022. doi: 10.3150/21-BEJ1410. URL <https://doi.org/10.3150/21-BEJ1410>.
- Ying Jin, Zhimei Ren, and Emmanuel J Candès. Sensitivity analysis of individual treatment effects: A robust conformal inference approach. *Proceedings of the National Academy of Sciences*, 120(6):e2214889120, 2023.
- Chancellor Johnstone and Bruce Cox. Conformal uncertainty sets for robust optimization. In *Conformal and Probabilistic Prediction and Applications*, pages 72–90. PMLR, 2021.
- Chancellor Johnstone and Eugene Ndiaye. Exact and approximate conformal inference in multiple dimensions. *arXiv preprint arXiv:2210.17405*, 2022.
- Nadja Klein. Distributional regression for data analysis. *arXiv preprint arXiv:2307.10651*, 2023.

- Nadja Klein and Thomas Kneib. Directional bivariate quantiles: a robust approach based on the cumulative distribution function. *AStA Advances in Statistical Analysis*, 104(2): 225–260, Jun 2020. ISSN 1863-818X. doi: 10.1007/s10182-019-00355-3. URL <https://doi.org/10.1007/s10182-019-00355-3>.
- Thomas Kneib, Alexander Silbersdorff, and Benjamin Säfken. Rage against the mean—a review of distributional regression approaches. *Econometrics and Statistics*, 2021.
- Arun Kumar Kuchibhotla. Exchangeability, conformal prediction, and rank tests. *arXiv preprint arXiv:2005.06095*, 2020.
- Daisuke Kurisu and Taisuke Otsu. Model averaging for global fréchet regression.
- Daisuke Kurisu, Yidong Zhou, Taisuke Otsu, and Hans-Georg Müller. Geodesic synthetic control methods for random objects and functional data. *arXiv preprint arXiv:2505.00331*, 2025.
- Jing Lei and Larry Wasserman. Distribution-free prediction bands for non-parametric regression. *Journal of the Royal Statistical Society: Series B: Statistical Methodology*, pages 71–96, 2014.
- Jing Lei, James Robins, and Larry Wasserman. Distribution-free prediction sets. *Journal of the American Statistical Association*, 108(501):278–287, 2013. doi: 10.1080/01621459.2012.751873. URL <https://doi.org/10.1080/01621459.2012.751873>.
- Jing Lei, Max G’Sell, Alessandro Rinaldo, Ryan J Tibshirani, and Larry Wasserman. Distribution-free predictive inference for regression. *Journal of the American Statistical Association*, 113(523):1094–1111, 2018.
- Jun Li and Regina Y Liu. Multivariate spacings based on data depth: I. construction of nonparametric multivariate tolerance regions. *The Annals of Statistics*, 36(3):1299–1323, 2008.
- Xun Li, Joyee Ghosh, and Gabriele Villarini. A comparison of bayesian multivariate versus univariate normal regression models for prediction. *The American Statistician*, 0(0):1–9, 2022. doi: 10.1080/00031305.2022.2087735. URL <https://doi.org/10.1080/00031305.2022.2087735>.
- Hang Liu, Xueqin Wang, and Jin Zhu. Quantiles, ranks and signs in metric spaces. *arXiv preprint arXiv:2209.04090*, 2022.
- Charles Lu, Yaodong Yu, Sai Praneeth Karimireddy, Michael Jordan, and Ramesh Raskar. Federated conformal predictors for distributed uncertainty quantification. In *International Conference on Machine Learning*, pages 22942–22964. PMLR, 2023.
- Helen Lu. *Data Augmentation and Conformal Prediction*. PhD thesis, Massachusetts Institute of Technology, 2023.
- Gábor Lugosi and Marcos Matabuena. Uncertainty quantification in metric spaces. *arXiv preprint arXiv:2405.05110*, 2024.

- Russell Lyons. Second errata to distance covariance in metric spaces. *The Annals of Probability*, 49(5):2668 – 2670, 2021. doi: 10.1214/20-AOP1504. URL <https://doi.org/10.1214/20-AOP1504>.
- Péter Major. On the invariance principle for sums of independent identically distributed random variables. *Journal of Multivariate Analysis*, 8(4):487–517, 1978. ISSN 0047-259X. doi: [https://doi.org/10.1016/0047-259X\(78\)90029-5](https://doi.org/10.1016/0047-259X(78)90029-5). URL <https://www.sciencedirect.com/science/article/pii/0047259X78900295>.
- Marcos Matabuena. Contributions on metric spaces with applications in personalized medicine. *PhD, Universidade de Santiago de Compostela*, 2022.
- Marcos Matabuena and Ciprian M Crainiceanu. Multilevel functional distributional models with application to continuous glucose monitoring in diabetes clinical trials. *arXiv preprint arXiv:2403.10514*, 2024.
- Marcos Matabuena and Alexander Petersen. Distributional data analysis of accelerometer data from the NHANES database using nonparametric survey regression models. *Journal of the Royal Statistical Society Series C: Applied Statistics*, 72(2):294–313, 02 2023. ISSN 0035-9254. doi: 10.1093/jrssc/qlad007. URL <https://doi.org/10.1093/jrssc/qlad007>.
- Marcos Matabuena, Alexander Petersen, Juan C Vidal, and Francisco Gude. Glucodensities: A new representation of glucose profiles using distributional data analysis. *Statistical Methods in Medical Research*, 30(6):1445–1464, 2021a. doi: 10.1177/0962280221998064. URL <https://doi.org/10.1177/0962280221998064>. PMID: 33760665.
- Marcos Matabuena, Pablo Rodríguez-Mier, Carlos García-Meixide, and Victor Leborán. Covid-19: Estimation of the transmission dynamics in spain using a stochastic simulator and black-box optimization techniques. *Computer methods and programs in biomedicine*, 211: 106399, 2021b.
- Marcos Matabuena, Paulo Félix, Carlos García-Meixide, and Francisco Gude. Kernel machine learning methods to handle missing responses with complex predictors. application in modelling five-year glucose changes using distributional representations. *Computer Methods and Programs in Biomedicine*, page 106905, 2022a.
- Marcos Matabuena, Paulo Félix, Ziad Akram Ali Hammouri, Jorge Mota, and Borja del Pozo Cruz. Physical activity phenotypes and mortality in older adults: a novel distributional data analysis of accelerometry in the nhanes. *Aging Clinical and Experimental Research*, pages 1–8, 2022b.
- Marcos Matabuena, Pedro Pugliesi Abdalla, Dalmo Roberto Lopes Machado, Lucimere Bohn, and Jorge Mota. Handgrip strength conditional tolerance regions suggest the need for personalized sarcopenia definition: an analysis of the american nhanes database. *Aging Clinical and Experimental Research*, 35(6):1369–1373, Jun 2023a. ISSN 1720-8319. doi: 10.1007/s40520-023-02398-8. URL <https://doi.org/10.1007/s40520-023-02398-8>.
- Marcos Matabuena, Paulo Felix, Marc Ditzhaus, Juan Vidal, and Francisco Gude. Hypothesis testing for matched pairs with missing data by maximum mean discrepancy: An application to continuous glucose monitoring. *The American Statistician*, 77(4):357–369,

2023b. doi: 10.1080/00031305.2023.2200512. URL <https://doi.org/10.1080/00031305.2023.2200512>.

Marcos Matabuena, Juan C. Vidal, Rahul Ghosal, and Jukka-Pekka Onnela. Deep learning framework with uncertainty quantification for survey data: Assessing and predicting diabetes mellitus risk in the american population, 2024.

Soundouss Messoudi, Sébastien Destercke, and Sylvain Rousseau. Ellipsoidal conformal inference for multi-target regression. In *Conformal and Probabilistic Prediction with Applications*, pages 294–306. PMLR, 2022.

Dimitri Meunier, Massimiliano Pontil, and Carlo Ciliberto. Distribution regression with sliced Wasserstein kernels. In Kamalika Chaudhuri, Stefanie Jegelka, Le Song, Csaba Szepesvari, Gang Niu, and Sivan Sabato, editors, *Proceedings of the 39th International Conference on Machine Learning*, volume 162 of *Proceedings of Machine Learning Research*, pages 15501–15523. PMLR, 17–23 Jul 2022. URL <https://proceedings.mlr.press/v162/meunier22b.html>.

Victor M Panaretos and Yoav Zemel. *An invitation to statistics in Wasserstein space*. Springer Nature, 2020.

Yash Patel, Declan McNamara, Jackson Loper, Jeffrey Regier, and Ambuj Tewari. Variational inference with coverage guarantees. *arXiv preprint arXiv:2305.14275*, 2023.

Alexander Petersen and Hans-Georg Müller. Fréchet regression for random objects with euclidean predictors. *The Annals of Statistics*, 47(2):691–719, 2019.

Alexander Petersen, Xi Liu, and Afshin A. Divani. Wasserstein  $F$ -tests and confidence bands for the Fréchet regression of density response curves. *The Annals of Statistics*, 49(1):590 – 611, 2021. doi: 10.1214/20-AOS1971. URL <https://doi.org/10.1214/20-AOS1971>.

Dimitris N Politis. Model-free prediction in regression. In *Model-Free Prediction and Regression*, pages 57–80. Springer, 2015.

Dimitris N Politis and Joseph P Romano. Large sample confidence regions based on subsamples under minimal assumptions. *The Annals of Statistics*, pages 2031–2050, 1994.

Rui Qiu, Zhou Yu, and Zhenhua Lin. Semi-supervised fréchet regression, 2024.

Yaniv Romano, Evan Patterson, and Emmanuel Candès. Conformalized quantile regression. *Advances in neural information processing systems*, 32, 2019.

Christof Schötz. *The Fréchet Mean and Statistics in Non-Euclidean Spaces*. PhD thesis, 2021.

Matteo Sesia and Emmanuel J. Candès. A comparison of some conformal quantile regression methods. *Stat*, 9(1):e261, 2020. doi: <https://doi.org/10.1002/sta4.261>. URL <https://onlinelibrary.wiley.com/doi/abs/10.1002/sta4.261>. e261 sta4.261.

Glenn Shafer and Vladimir Vovk. A tutorial on conformal prediction. *Journal of Machine Learning Research*, 9(3), 2008.

- Viral N Shah, Stephanie N DuBose, Zoey Li, Roy W Beck, Anne L Peters, Ruth S Weinstock, Davida Kruger, Michael Tansey, David Sparling, Stephanie Woerner, et al. Continuous glucose monitoring profiles in healthy nondiabetic participants: a multicenter prospective study. *The Journal of Clinical Endocrinology & Metabolism*, 104(10):4356–4364, 2019.
- Sukrita Singh, Neeraj Sarna, Munich Re, Yuanyuan Li, Yang Lin, Agni Orfanoudaki, and Michael Berger. Distribution-free risk assessment of regression-based machine learning algorithms. *arXiv preprint arXiv:2310.03545*, 2023.
- Aldo Solari and Vera Djordjilović. Multi split conformal prediction. *Statistics & Probability Letters*, 184:109395, 2022.
- Lisa Steyer, Almond Stöcker, and Sonja Greven. Elastic analysis of irregularly or sparsely sampled curves. *Biometrics*, 79(3):2103–2115, 2023.
- Sophia Sun. Conformal methods for quantifying uncertainty in spatiotemporal data: A survey. *arXiv preprint arXiv:2209.03580*, 2022.
- Jiaye Teng, Zeren Tan, and Yang Yuan. T-sci: A two-stage conformal inference algorithm with guaranteed coverage for cox-mlp. In *International Conference on Machine Learning*, pages 10203–10213. PMLR, 2021.
- Lori A Thombs and William R Schucany. Bootstrap prediction intervals for autoregression. *Journal of the American Statistical Association*, 85(410):486–492, 1990.
- Danielle C Tucker, Yichao Wu, and Hans-Georg Müller. Variable selection for global fréchet regression. *Journal of the American Statistical Association*, 0(0):1–15, 2021.
- Joni Virta. Spatial depth for data in metric spaces. *arXiv preprint arXiv:2306.09740*, 2023.
- Vladimir Vovk. Conditional validity of inductive conformal predictors. In *Asian conference on machine learning*, pages 475–490. PMLR, 2012.
- Vladimir Vovk, Alexander Gammerman, and Glenn Shafer. *Algorithmic learning in a random world*, volume 29. Springer, 2005.
- Vladimir Vovk, Iliia Nouretdinov, Valery Manokhin, and Alexander Gammerman. Cross-conformal predictive distributions. In *Conformal and Probabilistic Prediction and Applications*, pages 37–51. PMLR, 2018.
- Vladimir Vovk, Alexander Gammerman, and Glenn Shafer. Efficiency of conformal testing. In *Algorithmic Learning in a Random World*, pages 265–304. Springer, 2022.
- Kejin Wu and Dimitris N Politis. Bootstrap prediction inference of non-linear autoregressive models. *arXiv preprint arXiv:2306.04126*, 2023.
- Chen Xu and Yao Xie. Conformal prediction interval for dynamic time-series. In *International Conference on Machine Learning*, pages 11559–11569. PMLR, 2021.
- Chen Xu and Yao Xie. Conformal prediction for time series. *IEEE Transactions on Pattern Analysis and Machine Intelligence*, 2023.

- Mingzhang Yin, Claudia Shi, Yixin Wang, and David M Blei. Conformal sensitivity analysis for individual treatment effects. *Journal of the American Statistical Association*, pages 1–14, 2022.
- Margaux Zaffran, Aymeric Dieuleveut, Julie Josse, and Yaniv Romano. Conformal prediction with missing values. *arXiv preprint arXiv:2306.02732*, 2023.
- Qi Zhang, Bing Li, and Lingzhou Xue. Nonlinear sufficient dimension reduction for distribution-on-distribution regression. *arXiv preprint arXiv:2207.04613*, 2022.
- Yunyi Zhang. *Regression with complex data: regularization, prediction and bootstrap*. University of California, San Diego, 2022.
- Yunyi Zhang and Dimitris N Politis. Bootstrap prediction intervals with asymptotic conditional validity and unconditional guarantees. *Information and Inference: A Journal of the IMA*, 12(1):157–209, 06 2022. ISSN 2049-8772. doi: 10.1093/imaiai/iaac017. URL <https://doi.org/10.1093/imaiai/iaac017>.
- Hang Zhou and Hans-Georg Müller. Conformal inference for random objects, 2024. URL <https://arxiv.org/abs/2405.00294>.
- Yidong Zhou and Hans-Georg Müller. Network regression with graph laplacians. *Journal of Machine Learning Research*, 23(320):1–41, 2022. URL <http://jmlr.org/papers/v23/22-0681.html>.

## A Related Literature

Conformal inference techniques have been applied to various regression settings, including the estimation of the conditional mean regression function Lei et al. [2018], conditional quantiles Sesia and Candès [2020], and different quantities that arise from conditional distribution functions Singh et al. [2023], Chernozhukov et al. [2021a]. In recent years, multiple extensions of conformal techniques have emerged to handle counterfactual inference problems Chernozhukov et al. [2021b], Candès et al. [2023], Yin et al. [2022], Jin et al. [2023], heterogeneous policy effect Cheng and Yang [2022], reinforcement learning Dietterich and Hostetler [2025], federated learning Lu et al. [2023], outlier detection Bates et al. [2023], hypothesis testing Hu and Lei [2023], robust optimization Johnstone and Cox [2021], multilevel structures Fong and Holmes [2021], Dunn et al. [2022], missing data Matabuena et al. [2022a], Zaffran et al. [2023], and survival analysis problems Candès et al. [2023], Teng et al. [2021], as well as problems involving dependent data such as time series and spatial data Chernozhukov et al. [2021b], Xu and Xie [2021], Sun [2022], Xu and Xie [2023].

Despite the significant progress in conformal inference methods, there has been relatively little work on handling multivariate Johnstone and Ndiaye [2022], Messoudi et al. [2022] and functional data Lei et al. [2013], Diquigiovanni et al. [2022], Matabuena et al. [2021b], Dietterich and Hostetler [2022], Ghosal and Matabuena [2023]. In the case of classification problems, the first contributions to handle multivariate responses have also been recently proposed (see, for example, Cauchois et al. [2021]).

Zhang and Politis [2022], Wu and Politis [2023], Das et al. [2022], provide asymptotic marginal guarantees and, in certain cases, asymptotic results for the conditional coverage. The key idea behind these approaches is the application of resampling techniques, originally proposed by Politis et al. Politis and Romano [1994], to residuals or other score measures. Notably, these

methodologies are applicable regardless of the predictive algorithm being used, as emphasized by Politis [2015].

Bayesian methods are also an important framework to quantify uncertainty (see Chhikara and Guttman [1982]), which can also be integrated with conformal inference methods Angelopoulos and Bates [2023], Fong and Holmes [2021], Patel et al. [2023]. Gaussian response theory, including linear Gaussian and multivariate response regression models Thombs and Schucany [1990], Li et al. [2022], as a particular case, is a classical and popular approach. However, the latter techniques generally introduce stronger parametric assumptions in statistical modeling or include the limitation or difficulty in selecting the appropriate prior distribution in Bayesian modeling Gawlikowski et al. [2023]. The theory of tolerance regions gives another connection with the problem studied here Fraser and Guttman [1956], Hamada et al. [2004], which was generalized for the multivariate case with the notion of depth bands (see Li and Liu [2008]). However, a few conditional depth measures are available in the literature García-Meixide and Matabuena [2023]. Depth band measures for statistical objects that take values in metric spaces have recently been proposed Geenens et al. [2023], Dubey et al. [2022], Liu et al. [2022], Virta [2023] but only in the unconditional case.

### **A.0.1 Statistical modeling in metric spaces**

One of the most prominent applications of statistical modeling in metric spaces is in biomedical problems Matabuena [2022]. In personalized and digital medicine applications, it is increasingly common to measure patients' health conditions with complex statistical objects, such as curves and graphs, which allow recording patients' physiological functions and measuring the topological connectivity patterns of the brain at a high resolution level. For example, in recent work, the concept of "glucodensity" Matabuena et al. [2021a] has been coined, which is a distributional representation of a patient's glucose profile that improves existing methodology in diabetes research Matabuena et al. [2022a]. This representation is also helpful in obtaining better results with accelerometer data Matabuena and Petersen [2023], Ghosal et al. [2021b], Matabuena et al. [2022b], Ghosal and Matabuena [2023].

From a methodological point of view, statistical regression analysis of response data in metric spaces is a novel research direction Fan and Müller [2021], Chen et al. [2021], Petersen et al. [2021], Zhou and Müller [2022], Dubey and Müller [2022], Jeon et al. [2022,?], Kurisu and Otsu, Chen and Müller [2023]. The first papers on hypothesis testing Lyons [2021], Dubey and Müller [2019], Petersen et al. [2021], Fout and Fosdick [2023], variable selection Tucker et al. [2021], missing data Matabuena et al. [2023b], multilevel models Matabuena and Crainiceanu [2024], Bhattacharjee and Müller [2023], dimension-reduction Zhang et al. [2022], semi-parametric regression models Bhattacharjee and Müller [2021], Ghosal et al. [2023], semi-supervised algorithms Qiu et al. [2024] and non-parametric regression models Schötz [2021], Hanneke [2022], Bulté and Sørensen [2023], Bhattacharjee et al. [2023] have recently appeared.